

Distribution Agreement

In presenting this thesis as a partial fulfillment of the requirements for a degree from Emory University, I hereby grant to Emory University and its agents the non-exclusive license to archive, make accessible, and display my thesis in whole or in part in all forms of media, now or hereafter now, including display on the World Wide Web. I understand that I may select some access restrictions as part of the online submission of this thesis. I retain all ownership rights to the copyright of the thesis. I also retain the right to use in future works (such as articles or books) all or part of this thesis.

Alexandra Nazzari

April 15, 2018

Development of a responsive gene therapy to promote clearance of polyglutamine
aggregates

by

Alexandra Nazzari

Dr. Claire-Anne Gutekunst
Adviser

Department of Biology

Dr. Claire-Anne Gutekunst
Adviser

Dr. Nicole Gerardo
Committee Member

Dr. David Lynn
Committee Member

2019

Development of a responsive gene therapy to promote clearance of polyglutamine aggregates

By

Alexandra Nazzari

Dr. Claire-Anne Gutekunst

Adviser

An abstract of
a thesis submitted to the Faculty of Emory College of Arts and Sciences
of Emory University in partial fulfillment
of the requirements of the degree of
Bachelor of Sciences with Honors

Department of Biology

2019

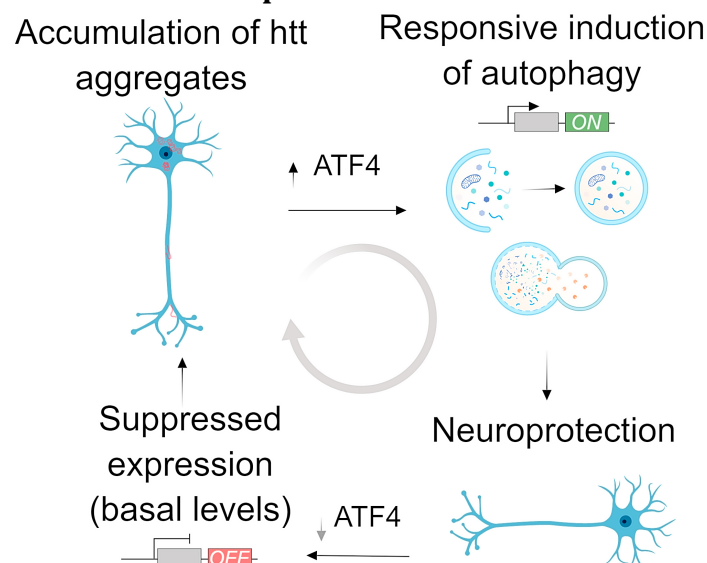
Abstract

Development of a responsive gene therapy to promote clearance of polyglutamine aggregates

By Alexandra Nazzari

Neurodegenerative diseases are devastating conditions characterized by protein toxicity and neuronal cell death, which is physically manifested as progressive cognitive and physical decline. Without a cure, current treatments focus on palliative care of symptoms. A responsive gene therapy targeted to neurodegenerative diseases, specifically Huntington's disease, is a promising tool to address the disease pathology at a cellular level with high specificity and temporal control. This responsive gene therapy construct was engineered to have a *sensing* modality in which activation is contingent on cellular status, neuronal stress induced by unfolded or misfolded proteins. When activated, the therapy construct is, subsequently, expressed. To target the mechanisms implicated in Huntington's disease (HD), the Unfolded Protein Response (UPR) was selected and its ability to detect misfolded proteins harnessed, using the stress-sensitive 5' untranslated region (UTR) of the activating transcription factor 4 (ATF4) gene. Upregulation of autophagy, the cell's natural mechanism for protein clearance, by increased expression of Beclin 1 (BECN1), was chosen as the therapy. This project entailed evaluating the components of our gene therapy in the context of endoplasmic reticular stress, assessing these constructs in a cellular model of HD and, ultimately, determining the efficacy of the responsive gene therapy's ability to clear polyglutamine aggregates.

Graphical Abstract



Development of a responsive gene therapy to promote clearance of polyglutamine aggregates

By

Alexandra Nazzari

Dr. Claire-Anne Gutekunst

Adviser

A thesis submitted to the Faculty of Emory College of Arts and Sciences
of Emory University in partial fulfillment
of the requirements of the degree of
Bachelor of Sciences with Honors

Department of Biology

2019

ACKNOWLEDGEMENTS

I would like to express my greatest appreciation to my advisor Dr. Claire-Anne Gutekunst, Angel Santiago-Lopez, and Dr. Ken Berglund for their support, guidance and mentorship throughout this project.

I would like to thank Dr. Claire-Anne Gutekunst for sharing her background and experience in Huntington's disease research, her expertise in the methodologies presented in this work and her dedication to my project and growth as a scientist.

My special thanks are extended to Angel Santiago-Lopez, who designed the concept for this responsive gene therapy. He guided me in my investigation of its application to Huntington's disease and provided valuable insight into the research process throughout this project.

I would like to thank Dr. Ken Berglund for his assistance in plasmid engineering and production as well as his advice in designing experiments.

I appreciate the support of our principal investigator, Dr. Robert Gross, who afforded me the opportunity to learn and conduct independent research in the laboratory.

I am grateful for my committee members, Dr. Nicole Gerardo and Dr. David Lynn, for dedicating their time and providing feedback on this thesis.

I would like to thank Dr. Shi-Hua Li (Emory, Department of Genetics), who kindly provided me with the Huntington Exon 1 plasmids that formed the foundation of my Huntington's disease model.

I wish to acknowledge the help provided by Xinping Huang (Emory Viral Vector Core) and Dr. Chen Wang (Dr. Zhigang He lab, Boston Children's Hospital Viral Core) in troubleshooting the adeno-associated viral vector production process.

TABLE OF CONTENTS

Abbreviations	1
Section 1: Background	2
Introduction.....	2
Huntington’s Disease.....	6
Sensing, ATF4 dependent sensing modality	10
Figure 1: UPR activation via the PERK pathway.....	11
Figure 2: Regulation of ATF4 translation.....	12
Molecular therapy, Beclin-1 Expression	14
Figure 3: Macroautophagy mechanism.....	14
Viral vectors in gene therapy.....	17
Responsive gene therapy	18
Figure 4: Gene therapy for unfolded protein regulation summary schematic.....	18
Section 2: Materials and Methods	20
Cell Culture.....	20
Plasmids	20
Table 1: Plasmid maps.	20
Transfection	22
UPR-Inducing Reagents	22
Imaging.....	22
Image analysis	23
Statistics.....	23
Immunocytochemistry	23
Adeno-associated virus production.....	24
Section 3: Results	25
HD Model.....	25
Figure 5: Huntingtin plasmid expression in HEK293 cells 32hr post-transfection.....	25
Figure 6: Time-lapse of HTT expression	26
Testing the ATF4 Sensor.....	26
Figure 7: <i>Sensing</i> construct.....	27
Figure 8: Differential expression of ATF4-GFP versus cGFP.....	27
Figure 9: TM-induced increase in ATF4 expression in HEK293	28
Figure 10: TM-induced increase in ATF4 expression blocked by PERKi in HEK293	29
ATF4 SENSOR IN HD Model.....	29
Figure 11: ATF4-GFP induction in response to HTT in HEK293 cells	30
Molecular therapy, Beclin-1 Expression	30
Figure 12: Beclin 1 Immunocytochemistry	31
Responsive Gene Therapy	31
Figure 13: ATF4-BECN1-GFP induction in response to HTT in HEK293 cells	32
Affect of BECN1 on HTT Expression.....	32
Figure 14: Effect of BECN1 treatment on HTT-Q20 expression in HEK293 cells.....	33
Figure 15: Effect of BECN1 treatment on HTT-Q150 expression in HEK293 cells	34
Figure 16: 1-way ANOVA.....	35
Effective transduction of neuronal cultures with ATF4 sensor construct	35
Figure 17: Tunicamycin induction of AAV2-ATF4-GFP construct in neuronal culture.....	36
Figure 18: Adeno-associated virus	36

Section 4: Discussion	37
Section 5: Conclusion	40
Section 6: Works Cited	41
Appendix A: Cell profiler image analysis	44
Appendix B: Statistical Analysis.....	46

ABBREVIATIONS

HD: Huntington's disease
PQC: Protein Quality Control system
SCA: spinocerebellar ataxias
polyQ: polyglutamine
CAG: trinucleotide repeat (expanded in HD)
HTT: Huntingtin protein
IT-15: Interesting Transcript-15
mHTT: Mutant Huntingtin
BECN1: Beclin 1 (Bcl-2-interacting myosin-like coiled-coil protein, also known as Atg6: autophagy-related gene 6)
ER: endoplasmic reticulum
UPR: unfolded protein response
ATF4: Activating Transcription Factor 4
uORF: Upstream Open Reading Frame
UTR: Untranslated Region
GTUPR: Gene Therapy for Unfolded Protein Regulation
UPS: ubiquitin–proteasome system
CMA: chaperone-mediated autophagy
ERAD: ER-associated degradation
PERK: protein kinase-like endoplasmic reticulum kinase
ATF6: activating transcription factor 6
IRE1: inositol requiring kinase 1
BiP: binding immunoglobulin protein (GRP78: glucose-regulated protein 78)
eIF2 α : alpha-subunit of eukaryotic initiation factor 2
P-eIF2 α : Phosphorylated alpha-subunit of eukaryotic initiation factor 2
GTP: guanosine
Met-tRNA: Methionated Transfer Ribonucleic acid
GDP: guanine diphosphate
CHOP: CCAAT-enhancer-binding protein homologous protein
GADD34: Growth Arrest And DNA-Damage-Inducible 34
GADD34-PP1: Growth Arrest And DNA-Damage-Inducible 34 -Protein Phosphatase 1
AVV: Adeno-associated virus
HEK293: Human Embryonic Kidney cell
DMEM: Dulbecco's modified Eagle's medium
FBS: fetal bovine serum
GFP: Green Fluorescent Protein
cGFP: Constitutively expressed GFP
CBA: Chicken β -actin promoter
TM: Tunicamycin
ds-RED: Red Fluorescent Protein
PERKi: Protein kinase-like endoplasmic reticulum kinase inhibitor
hSyn: human synapsin I

SECTION 1: BACKGROUND

INTRODUCTION

As the average human lifespan increases, there has been a corresponding rise in the prevalence of age-related neurodegenerative diseases, including Alzheimer's disease, Parkinson's disease, Huntington's disease (HD) and amyotrophic lateral sclerosis. These devastating diseases cause progressive motor deficits and psychological decline, which, on a molecular level, appears to stem from protein toxicity of a disease-specific identity that affects particular brain regions. The mechanisms of toxicity are complicated; misfolding, fragmentation, aggregation and accumulation hinder many cellular processes including transcriptional regulation, mitochondrial function, axonal transport and the functioning of Protein Quality Control (PQC) systems. Such global dysfunction in the neuron, ultimately, induces cellular death.¹

Despite efforts to prevent, slow and cure these diseases, most of the current treatments are only able to address patients' symptoms, mainly the motor abnormalities, specifically known as chorea in HD.² Hence, a molecular approach in the form of a responsive gene therapy could be instrumental in addressing the underlying pathology.

HD is a progressive neurological condition with genetic underpinnings. It is in a family of nine polyglutamine disorders, including dentatorubral-pallidoluysian atrophy, spinal-bulbar muscular atrophy, and six forms of spinocerebellar ataxias (SCA1, 2, 3, 6, 7, 17). HD is an autosomal dominant genetic condition found on the short arm of human chromosome four.³ The elongated trinucleotide repeat unit, CAG, is the common link, which translates into a mutant protein with an extended polyglutamine (polyQ) tract.⁴ In HD, the mutation occurs in the huntingtin or IT15 gene, leading to a polyQ repeat in the amino-terminal region of the huntingtin

protein (HTT). In individuals with more than thirty-six CAG repeats, the HD phenotype is manifested at an average age of onset of forty years. Fewer than thirty-six repeats is considered normal.⁵ Beyond this, a longer repeat sequence has been correlated with earlier onset of the disease.⁶

The HD pathology is of particular interest because the genetic cause is present from birth; however, symptomatically, neurodegeneration does not present until later in life. Additionally, HTT is ubiquitously expressed throughout the body and necessary for development; yet, the effect of mutant huntingtin protein (mHTT) appears to selectively induce neuronal cell death, first, in the striatum. Less emphasized effects of mHTT are being uncovered as researchers study the effects of mHTT on muscle, blood and adipose tissue.⁷

Several theories exist to explain the late onset of the disease phenotype and the selective cell death. First, the functional ability of the PQC system, including the ubiquitin-proteasome, chaperones, and autophagy, may decline with age. Furthermore, there may be a limit to the cell's ability to process the protein, a threshold that is reached later in life. Additionally, environmental triggers and or epigenetic factors may influence the disease onset and progression.¹

As post-mitotic cells, neurons may also be more sensitive to the effects of mHTT, while, in certain subpopulations, heightened vulnerability may be derived from differences in mechanisms of regulation and signaling related to the HTT protein.⁷ Evidence that shows the cell's inherent protein clearance abilities decline with both age and in the context of neurodegenerative diseases, including HD,⁸ suggests autophagy may be an intriguing therapeutic target.

Autophagy is a cytoprotective and adaptive mechanism for the cell to partition off and degrade misfolded proteins and damaged organelles, which yield material that can then be

recycled. The cell forms an autophagosome, a double-membraned compartment around the aberrant material. After maturation and transport, the autophagosome fuses with a lysosome, releasing its degradative enzymes, denaturing and disassembling the proteins. Macroautophagy is a specific subtype that, theoretically, could promote the degradation of large polyglutamine aggregates. However, in HD, autophagy is impaired at several steps within the pathway. Notably, there is a downregulation and sequestration of Beclin 1 (BECN1), a key regulator of autophagy. In addition to BECN1 being sequestered within aggresomes, the extended polyQ region of mHTT competes with the shorter polyQ binding region of Ataxin-3. Ataxin-3 normally binds to BECN1 and has deubiquitinase activity that prevents the degradation of BECN1. When mHTT interacts directly with BECN1, it prevents the deubiquitination and increases degradation, which results in lower levels of autophagy induction. Modulation of BECN1 expression appears to be beneficial in numerous polyQ diseases. Increased BECN1 expression seems to compensate for the abnormal protein-protein interactions, restoring autophagy and improving the phenotype *in vitro* and *in vivo*.⁹

While the goal is to delay or even prevent neurodegeneration, by promoting clearance of mutant proteins, polyglutamine aggregates, overstimulation of autophagy is also detrimental to the cell.¹⁰ A responsive or self-regulatory gene therapy addresses this issue and introduces high spatiotemporal control.

This therapy construct is designed under the control of a *sensing* modality, which modulates its expression based on a certain cellular status, in this case, neuronal stress. Neurons have intrinsic mechanisms for maintaining homeostasis under stress. One such mechanism involves the endoplasmic reticulum (ER), which contains embedded kinases that serve as intracellular sensors and capture stress signals associated with protein dysregulation. This, in

turn, activates gene expression through the signaling pathway known as the unfolded protein response (UPR), shown to be upregulated in HD.¹¹ The UPR functions to improve protein-folding machinery to clear misfolded proteins and reduce bulk translation. Select genes are upregulated in these conditions. One such gene is activating transcription factor 4 (ATF4), which has a stress-sensitive leader sequence.

The leader sequence of the ATF4 gene contains two upstream open reading frames (uORF). Under normal conditions, an inhibitory, out-of-frame uORF prevents translation of ATF4. Conversely, when the UPR is activated, the transcript is translated. We capitalized upon this innate mechanism, using 5' untranslated region (UTR) of the ATF4 gene, the leader sequence, to control the translation of a reporter gene and our therapy construct.

This responsive gene therapy for unfolded protein regulation (GTUPR) was designed to target neurodegeneration at a molecular level, focusing on protein toxicity. Using the adaptive mechanism of the UPR, the leader sequence of the ATF4 gene modulates expression of therapy construct, inducing expression only in stress conditions, when unfolded proteins are present in the cell. BECN1, a key regulator of autophagy, was chosen as a therapy to promote the clearance of polyglutamine protein aggregates.

HUNTINGTON'S DISEASE

Huntington's disease was named after George Huntington, a physician who extensively described, in 1872, the motoric presentation of the disease, otherwise known as chorea. Derived from the greek word for "dance," chorea manifests as jerky, abnormal and involuntary movements. About a century later in the 1980s, Nancy Wexler, a psychoanalyst, then attempted to link 18,000 cases of the disease into a common pedigree. In 1983, a team led by James Gusella, at Harvard Medical School and Massachusetts General Hospital localized the HD genetic locus to the short-arm of chromosome 4. The gene was then sequenced in 1993 by a large collaboration of researchers, known as the Huntington's Disease Collaborative Research Group.¹² The protein that is expressed from this gene is designated HTT and the mutant form mHTT contains the elongated polyQ tract at the N-terminus of the protein. Extensive research has been conducted to characterize the molecular nature of both normal HTT and mHTT, with hopes of developing a strategy to treat the disease.

In the non-HD population, 9-35 CAG repeats are considered healthy, with a median of 17-20 repeats. A rare version of late-onset HD is caused by 36-39 repeats, whereas, more than 40 repeats are defined as HD. Greater than 75 repeats induces the early onset, juvenile form of HD.⁵

Normal HTT is a large protein containing about 3,144 amino acids. At the N-terminus of the protein, there are 17 amino acids preceding the variable polyQ region. This region forms an amphipathic alpha-helix that modulates the protein's interaction with the membrane of the endoplasmic reticulum.^{5,13,14} The polyQ region is followed a proline-rich domain. Together, this constitutes the exon 1, the first coding region of the transcript. Interestingly, HTT exon 1 has been poorly conserved, evolutionarily, where mammals, specifically humans, developed an expanded polyQ stretch with high inter-individual variability in number of CAG repeats.⁵ Hence, the majority of studies have focused on exon 1.

In each of the 9 polyQ diseases, the disease-specific protein contains an elongated glutamine tract, which correspondingly causes neurodegeneration in select brain regions. This implies a difference in function of each protein and a varying vulnerability of the neuronal subpopulations. HD primarily affects the medium spiny neurons of the striatum and the striatal neurons that project to the cortex.⁵ The post-mitotic nature of the neurons and their extremely high-energy demands are hypothesized to be the reasons for their increased sensitivity. Why the neurodegeneration is largely localized to the striatum is an intriguing question: a possible explanation is HTT's mechanism of action in this subpopulation is somehow altered, which leads to an increase protein toxicity for these specific cells.⁹

To address how mHTT is actually causing protein toxicity, scientists have attempted to classify HD as a gain of function or loss of function phenomenon; however, this is still under debate, likely because the mechanisms as well as the various and diverse protein-protein interactions of normal HTT are still being elucidated. The widespread cellular dysfunction in HD also supports the multifaceted nature of this protein. Dysfunction in cells showing the disease phenotype have been found both in *in vitro* and *in vivo* models to stem from multiple subcellular compartments: the nucleus, mitochondria, endoplasmic reticulum, axonal transport system. Overall, HTT seems to be a central scaffolding protein,⁵ which, as a result, has numerous binding interactions and guides and perhaps coordinates cellular functions.

Just as wild-type HTT has many functions, mHTT interferes in several pathways, resulting in widespread dysfunction. Towards the N-terminus of normal HTT protein, it contains a nuclear export signal, allowing it to act as a transcription factor, altering gene expression.⁵ With an expanded polyQ, the fragment enters the nucleus and forms internuclear aggregates sequestering critical transcription factors.¹ Blocking nuclear entry of these mHTT fragments

greatly reduces toxicity.⁴ Additionally, mHTT increases reactive oxygen species and causes mitochondrial dysfunction, which is particularly detrimental to neurons with their high-energy demands.

Although mHTT is present and expressed in the disease form starting from birth, the symptoms of the disease do not typically begin until the individual's mid-30s. This suggests the cells may be equipped to handle the mutant protein to a certain extent. Indeed, cells have several innate mechanisms to identify, alter and degrade misfolded proteins. This is collectively referred to as the Protein Quality Control (PQC) system, which includes the ubiquitin–proteasome system (UPS - ubiquitin tags a protein for degradation by proteases), chaperone-mediated autophagy (CMA - chaperones, molecular folding machines, attempt to correctly fold native proteins and refold misfolded proteins or target them for degradation), macroautophagy (vesicles are formed around misfolded proteins or damaged organelles and lysosomes full of catabolic enzymes fuse to breakdown and recycle the components), and ER-associated degradation (ERAD).^{1,15} These systems, as a whole, are found to have decreased activity with age⁸ and are impaired in a range of neurological conditions.¹⁵

In HD, mHTT is degraded by the UPS and, furthermore, aggregates in post-mortem brain tissue often colocalize with proteasomal proteins including heat shock proteins and ubiquitin.⁴ Additionally and notably, macroautophagy, commonly and further referred to as autophagy, also degrades mHTT, including large aggregates, although is impaired in HD. Decreased autophagy functioning likely stems from changes to the normal role of wild-type HTT in both autophagy directly as well as axonal transport. NonHD HTT regulates both anterograde and retrograde transport of substances, including organelles and autophagosomes.⁵

Several studies indicate that targeting and inducing autophagy, promoting the cell's own clearance of proteins, via various pharmacological activation methods can alleviate some of the stress and toxicity associated with the protein aggregation and accumulation seen in neurodegenerative diseases.¹⁶

SENSING, ATF4 DEPENDENT SENSING MODALITY

In order to deliver an effective gene therapy for HD, and more generally diseases of unfolded proteins, timing and dosage is crucial. If autophagy is upregulated ubiquitously, at too high a level, or if misfolded proteins are not present, then a buildup of autophagosomes is likely and may cause even more harm. Hence, the responsive element is central to the design of this gene therapy. The goal was to design a system that was autonomous, a system where the cell's biochemical status *informs* and modulates the expression of the therapy.

Conditions like HD, Parkinson's, and Alzheimer's disease are linked by a buildup of aberrant proteins, which all trigger the UPR.¹⁷ Three "stress sensors" are situated in the ER membrane: RNA-activated protein kinase-like endoplasmic reticulum kinase (PERK), activating transcription factor 6 (ATF6), and inositol requiring kinase 1 (IRE1).¹⁸ In the presence of misfolded protein in the ER lumen, these kinases are activated. PERK and IRE1 dimerize and phosphorylate downstream targets.

The PERK pathway is of particular interest and was used to design the sensing modality of this responsive gene therapy. Binding immunoglobulin protein (BiP, also known as glucose-regulated protein 78, GRP78) is a protein localized to the ER lumen and bound to PERK. Improperly folded proteins usually lack glucose moieties and have exposed hydrophobic residues, which enables their interaction with the luminal portion of PERK-bound BiP. BiP dissociates from the membrane and binds to misfolded proteins, allowing the PERK proteins to dimerize, autophosphorylate and phosphorylate the alpha-subunit of eukaryotic initiation factor 2 (eIF2 α).¹¹ Phosphorylated eIF2 α (p-eIF2 α) levels are critical in regulation translation of mRNA in neurons. P-eIF2 α levels have been shown to be increased in models of HD.^{19,20}

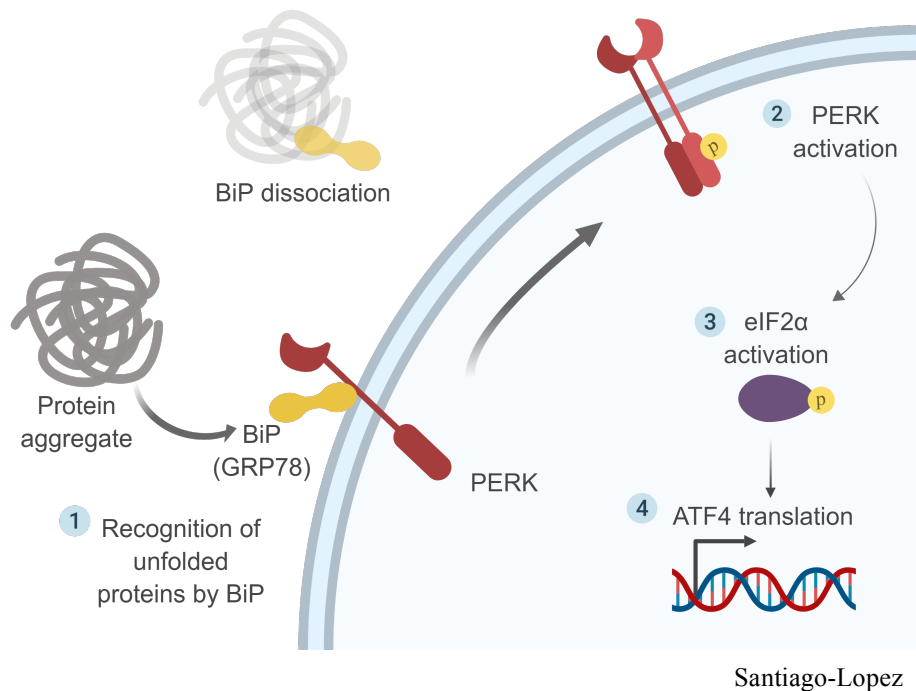


Figure 1: UPR activation via the PERK pathway.

eIF2, under normal conditions, binds guanosine triphosphate (GTP) at the gamma subunit, which binds to an activated methionated transfer RNA (met-tRNA), forming the ternary complex. This complex is required for the initiation of translation. When eIF2 is phosphorylated at the alpha-subunit, conversion of guanosine diphosphate (GDP) to GTP is inhibited, effectively decreasing ternary complex formation and, in turn, reducing bulk translation in the cell.¹⁹ This adaptive mechanism decreases the production of new proteins so that the cell is better able to address misfolded proteins.

While bulk translation is decreased, there are select genes that are upregulated in these stress conditions. These genes encode transcripts with stress-sensitive upstream open reading frames (uORFs). The decreased ternary complex allows the ribosomes to scan through inhibitory UTRs and reach coding regions that are typically not read if ternary complex is abundant.¹⁹

One gene that shows such increased translation, under stress conditions, is ATF4. The ATF4 transcript contains a 5'-proximal uORF1, three codons long, and a second ORF2, 59

codons long, that overlaps out-of-frame with the ATF4 coding region.²¹ uORF1 is a positive element that promotes downstream re-initiation of translation. Under unstressed conditions, abundant ternary complex present, translation is reinitiated at uORF2 and the ATF4 gene product is not translated (see Figure 2 schematic). Conversely, under stressed conditions, ternary complex is scarce, which causes the ribosome to scan through the initiation region of uORF2, promoting the translation of the ATF4 protein.²² The expression of the protein is, thus, contingent upon the amount of ternary complex, resulting from p-eIF2 α levels, and originating from the kinases detecting stress at the ER membrane.

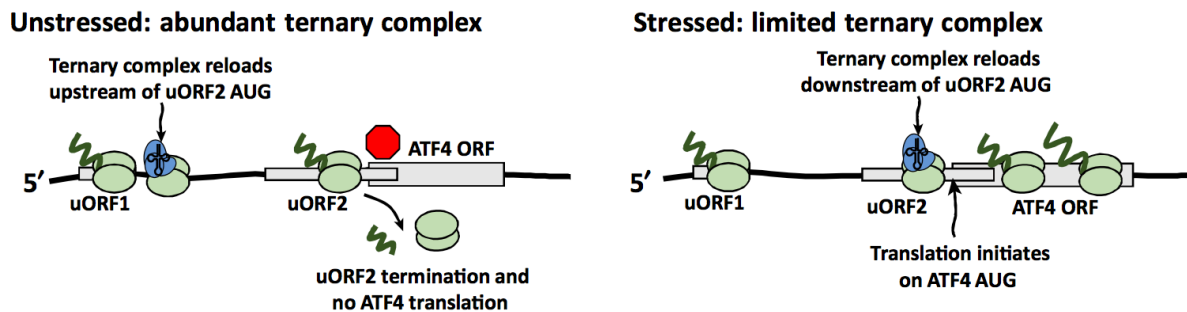


Figure from: Moon, Trends in Molecular Medicine. 2018.

Figure 2: Regulation of ATF4 translation. During UPR-induced stress, ternary complex is limited and, hence, the ATF4 translation is increased.

The UPR is sophisticated, in that, the adaptive mechanisms are activated in the presence of unfolded protein; but, with excessive or chronic stress, this signaling can also induce apoptotic pathways. Notably, ATF4 upregulates CCAAT-enhancer-binding protein homologous protein (CHOP), a downstream product of PERK, that orchestrates cell death.²³

Similar to ATF4, Growth Arrest And DNA-Damage-Inducible protein 34 (GADD34) transcripts also contain two uORFs that are responsive to stress. This gene triggers negative feedback regulation. The protein complex GADD34-Protein Phosphatase 1 (PP1) functions to

dephosphorylate eIF2 α , suppressing the PERK/eIF2 α signaling pathway.¹⁸ This reversibility helps to restore translation following the resolution of the UPR.²⁴

This responsive GTUPR is based on the selective translation of ATF4, leveraging the sensing and transducing actions of PERK signaling to control the expression of the therapy construct.

MOLECULAR THERAPY, BECLIN-1 EXPRESSION

In HD, autophagy and proteasomal degradation are involved in the clearance of mHTT; however, once mHTT oligomerizes and aggregates, this mass of protein is likely to only be degraded by autophagy. Blocking autophagy has been shown to decrease cell viability and increase aggregation, while promoting autophagy enhances protein clearance.^{9,25} This relationship suggests that targeting autophagy may be a beneficial strategy against diseases with prominent protein toxicity, such as neurodegenerative conditions.

Macroautophagy, referred to as autophagy, is an inherent pathway that a cell employs to recycle damaged organelles and proteins. First to form is an isolation membrane, a lipid bilayer, which is the foundation of the phagophore. The membrane engulfs its cargo, such as aggregated protein, forming the autophagosome. The autophagosome then fuses with a lysosome, introducing proteases that breakdown the contents.²⁶ There are several key steps for the initiation, nucleation, extension of the phagophore as well as the fusion with the lysosome and degradation, are impaired with age and in disease processes.

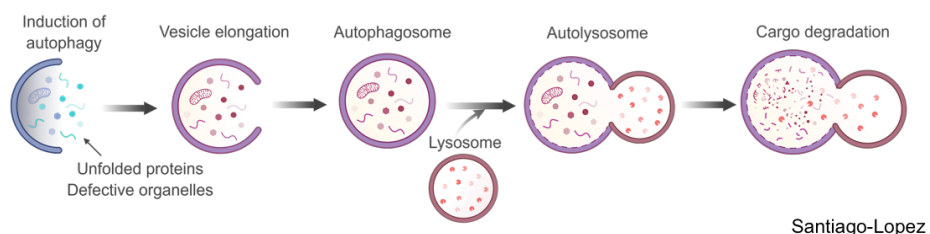


Figure 3: Macroautophagy mechanism

Interestingly, thirty genes necessary for autophagy have been identified, of which several have been found to be decreased in the brain with increasing age, including Atg5, Atg7, and BECN1.^{8,27} Furthermore, the absence of these autophagy-associated genes in neurons induced

age-dependent neurodegeneration with characteristic cellular inclusions of protein aggregates.^{28,29}

BECN1, (Bcl-2-interacting myosin-like coiled-coil protein), also known as autophagy-related gene 6 (Atg6), was discovered and named after its interaction with anti-apoptotic B-cell lymphoma-2 (Bcl2) and is a key regulator of autophagy. It controls the formation of phosphatidylinositol 3-phosphate and the recruitment of autophagy proteins to form the autophagosome.³⁰ Decreased BECN1 and its sequestration in aggresomes has been reported in HD.³⁰

Modulation of BECN1 expression has been tested for the treatment of Alzheimer's disease, Parkinson's disease and HD. Introduction of BECN1 using lentiviral vectors in a rat model of SCA3, another polyQ disorder, improved motor symptoms.^{9,31,32} BECN1 expression also showed improvements in cell culture models of HD in primary neurons.^{9,33} Deletion of the HTT polyQ stretch in mice enhances autophagy and results in increased longevity.^{5,34}

In addition to autophagy genes being downregulated with age, the autophagy pathway is significantly impaired in HD. One consequence of the elongated polyglutamine tract is abnormal protein-protein interactions. Ataxin-3 interacts with BECN1 via a polyQ domain, and through its deubiquitinase properties prevents the degradation of BECN1. Full-length mHTT competes with this binding domain and increases proteasomal degradation of BECN1. mHtt also impairs cargo loading and can result in the formation of empty autophagosomes.³⁵

Pharmacological modulation of autophagy *in vitro* and in preclinical animal studies has been shown to effectively reduce protein burden and attenuate neuron loss in a range of neurodegenerative diseases.³⁶⁻³⁸

Induction of autophagy is a promising strategy to increase the clearance of polyglutamine aggregates, in turn, slowing the progression of the disease and decreasing symptoms. In order for induction of autophagy to be therapeutic, its activation must be highly regulated. Overactivation of autophagy will result in excessive formation of autophagosomes and, at high enough levels, may trigger cell death. Hence, a responsive gene therapy model that is able to alter levels of expression, and thus, induction of autophagy, is a crucial component to preventing excessive degradation and re-establishing homeostasis in the neurons.

VIRAL VECTORS IN GENE THERAPY

When designing a gene therapy to target the central nervous system, the method of delivery is critical for the effective introduction of the construct to cells. Viral vectors are extremely powerful tools to target neuronal populations.

Adeno-associated viral (AAV) vectors take advantage of the low human pathogenicity of this family of parvoviruses. There are more than a dozen serotypes (AAV1-AAV13) of AAVs providing a range of infectability for various cell types. Viral capsid engineering has also been successful in targeting specific cell populations. The virus' highly tunable shell is used to encapsulate a construct of interest and act as an efficient delivery system. The high specificity and ability to engineer the viral capsids to target specific cellular receptors make AAVs a valuable tool for biomedical applications. Additionally, using cell-specific promoters, gene expression in specific neuronal subpopulations can be further tailored on a transcriptional level.³⁹

The long-term gene expression achieved with AAVs would also be ideal to modulate autophagy over a span of several years, during the progression of neurodegeneration.

RESPONSIVE GENE THERAPY

Introducing the responsive element to this gene therapy creates a self-sufficient delivery system, in which cellular status *informs* the output, titrating the level of treatment to the disease state at a cellular level.

We have designed our gene therapy construct so that levels of p-eIF2 α are a proxy for the presence of misfolded proteins in the cell and serve to regulate the translation of our introduced therapy construct (Figure 4).

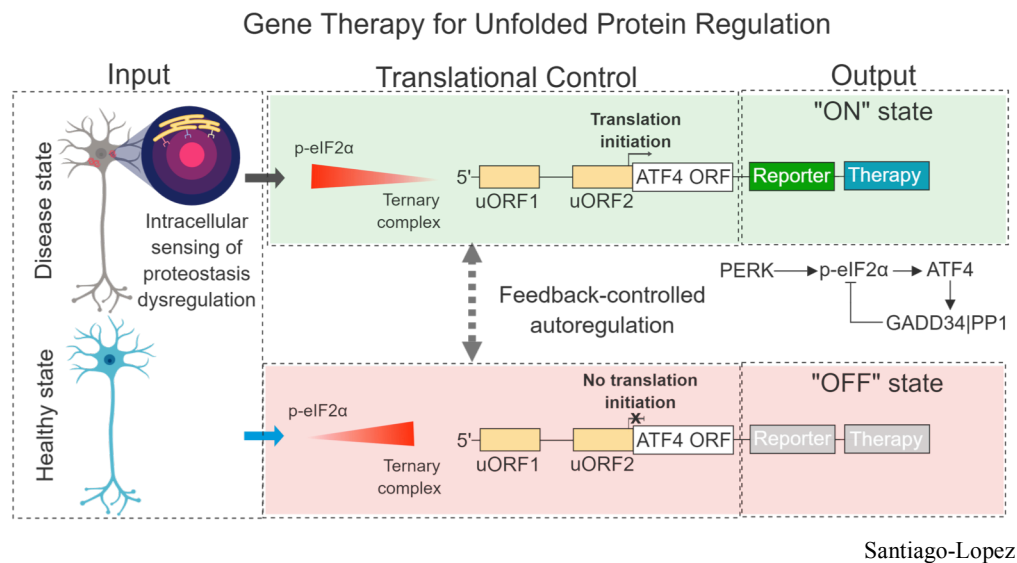


Figure 4: Gene therapy for unfolded protein regulation summary schematic

Utilizing a closed-loop system addresses the challenge of regulating dosing when introducing a gene therapy. The use of a self-regulating gene therapy has been extensively investigated for the application of glucose-responsive insulin delivery systems to treat diabetes.⁴⁰ Additionally, many other molecules are being considered in the design of responsive gene therapy systems to treat a range of disorders. For example, stimuli including cytokines,^{41,42} uric acid,⁴³ hormones,⁴⁴ and others^{45,46} are under consideration to control the expression of gene

therapy constructs. The use of a responsive gene therapy based on the 5' UTR of ATF4 represents a novel approach to controlling gene therapies targeting neurodegenerative diseases.

SECTION 2: MATERIALS AND METHODS

CELL CULTURE

Human embryonic kidney cell line (HEK293, ATCC[®] CRL-3216[™]): HEK293 cells were maintained in Dulbecco's modified Eagle's medium (DMEM) high glucose supplemented with 10% fetal bovine serum (FBS) and 1% Penicillin-Streptomycin at 37°C, 5% CO₂.

Primary mouse neuronal culture: cultures were established from embryonic (E18) mouse cortical tissue using the papain dissociation kit (for extended protocol see Santiago-Lopez, 2018.⁴⁷) and plated in cell culture dishes. Neuronal cultures were maintained with Neurobasal medium supplemented with B27 (2 mM), 1 µg/mL gentamicin, Glutamax[™]-I (2 mM), 1% Penicillin-Streptomycin.

PLASMIDS

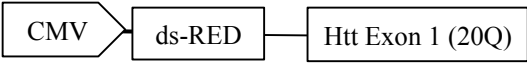
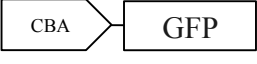
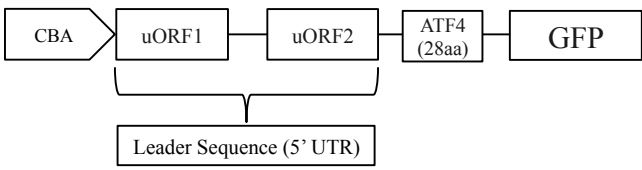
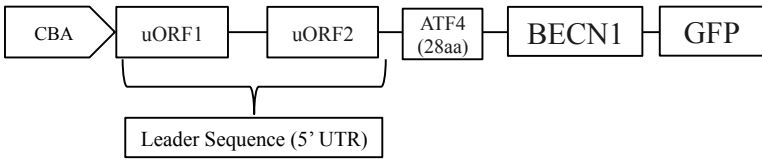
Htt Q20	
Htt Q150	
GFP	
ATF4-GFP	
Beclin 1-GFP	
ATF4-Beclin 1- GFP	

Table 1: Plasmid maps.

The DNA plasmids were produced by Dr. Ken Berglund using conventional molecular biology with restriction enzymes (RE) and ligase. To generate a control viral vector with the GFP gene followed by the self-cleaving porcine teschovirus-1 2A sequence (P2A) and multiple cloning sites (MCS), the DNA sequence flanked by the BsrGI and BglII RE sites was synthesized (gBlock gene fragments, Integrated DNA Technologies). The DNA was ligated into the corresponding BsrGI and BglII sites in pAAV/CBA::GFP-2A-myc-C3 previously made in the lab. To improve mRNA stability, the woodchuck hepatitis virus posttranscriptional regulatory element (WPRE) in pAAV/EF1 α ::DIO-SwiChR/CA-TS-EYFP (Addgene plasmid #: 55631; a gift from Karl Deisseroth) was cut with EcoRV and BglII and ligated into the BglII site after the transgene. The incompatible 3' BglII cut in the backbone was blunt-ended with Klenow, resulting in pAAV/CBA-GFP. The regulatory domain of human activating transcription factor 4 (ATF4; 5' untranslated region and the first 28 amino acids of the coding region) flanked by the EcoRI and AgeI RE sites was similarly synthesized and ligated into the corresponding sites in-frame with 4 extra amino acids (PVAT) in front of the GFP gene, resulting in pAAV/CBA::ATF4-GFP. To generate the two vectors with mouse Beclin 1 fused with GFP, the gene in pBeclin-HA (Addgene plasmid #: 46993; a gift from Kunlian Guan) was PCR-amplified with the primers with AgeI RE sites and ligated in-frame with 2 extra amino acids (PV) into the corresponding RE sites in the two vectors, resulting pAAV/CBA::BECN1-GFP and pAAV/CBA::ATF4-BECN1-GFP. The correct sequences were confirmed by RE digestion analyses and DNA sequencing.

Huntingtin plasmids derived from the human exon 1 of the huntingtin gene, with 20 or 150 CAG repeats respectively, were tagged with ds-red fluorescent protein (dsRed-HTT-exon 1-

Q20 and dsRed-HTT-exon 1-Q150) (a gift from Dr. Shi-Hua Li, Emory University, Department of Human Genetics).

Transfection

LipofectamineTM3000 (ThermoFisher Scientific) reagent was used for transfections. Transfections were performed in 96-well cell culture plates according to ranges suggested in the ThermoFisher protocol. 5ul of transfection mixture was added per well. 0.25ul P3000 reagent and 0.25ul of LipofectamineTM3000 was used per well. 0.125ug of DNA per plasmid was add to the P3000 reagent in OptiMEM, incubated for 5 minutes. This was then added to the LipofectamineTM3000 mixture and incubated for 20 minutes before being added to the cells.

UPR-Inducing Reagents

Tunicamycin (Sigma-Aldrich) and PERK inhibitor (Sigma-Aldrich) were dissolved in DMSO and diluted in PBS to the desired concentration.

Imaging

The Biotek Cytation 5 system was used for automated image acquisition. For each experiment, each condition was tested in triplicate (n=3). Either a 2x2 imaging grid, 4 total images, or 3x3 imaging grid, 9 total images, were taken per well.

For imaging, the DAPI filter cube/LED (Part #:1225100, EX:377/50, EM:447/60, Mirror:409, LED Part #:1225007, 365nm), GFP filter cube (Part #:1225101, EX:469/35, EM:525/39, Mirror:497, LED Part #:1225001, 465nm), Texas Red filter cube (Part #:1225102, EX:586/15, EM:685/40, Mirror:605, LED Part #:1225002, 590nm), and CY5 filter cube (Part #:1225105, EX:628/40, EM:685/40, Mirror:660, LED Part #:1225005, 623nm), 10x and 20x

Olympus Plan Fluorite objective were used. During kinetic experiments, the Laser Autofocus cube (part #: 1225010) was used to focus in each channel.

Image analysis

Cell profiler image analysis software (Broad Institute)⁴⁸ was used to analyze fluorescent images. Using the software's segmentation algorithms, specifically the 3-class Otsu method, GFP and ds-RED objects were identified and further quantified for size and intensity on a per cell and image basis (Appendix A).

Statistics

The mean integrated intensity of ds-RED per object is indicative of the amount of huntingtin expression in the cells and used to compare treatments outcomes. This was analyzed using a 1-one ANOVA with Tukey's adjustments, in GraphPad Prism (details shown in Appendix B), at the endpoint of 59 hours post-transfection. All groups were expressing the ATF4-BECN1 construct. The three groups included no HTT, HTT-Q20, and HTT-Q150. An alpha value of 0.05 was used to determine significance.

Immunocytochemistry

Cells were fixed in 4% paraformaldehyde (PFA) in PBS for 15 min and processed for immunocytochemistry (ICC) using mouse anti-BECN1 antibody (Santa-Cruz). Briefly, cells were permeabilized with 0.01% Triton X-100 in PBS for 5 min, (Sigma-Aldrich, St Louis, MO) in PBS for 5 min, blocked in 4% normal donkey serum (NDS, Jackson ImmunoResearch Laboratories, West Grove PA) for 30 min and incubated with mouse anti-BECN1 antibody (Santa-Cruz) used at 1:200 in 2% NDS in PBS overnight. After several washes, the cells were incubated in Alexa Fluor[®] 647 donkey anti-mouse IgG secondary antibody (ThermoFisher

Scientific; Cat. R37115) in PBS for 1hr. A DAPI counterstain was also added to visualize the nuclei. Cells were imaged using an inverted Leica DMIRE2 scope equipped with a QImaging Retiga EXi camera and Simple PCI acquisition software. The captured images were stored and processed using FIJI (ImageJ) software.

Adeno-associated virus production

AAV2 capsid, derived from the AAV2/2 RC plasmid (UPenn vector facility) was used to generate viral vectors, according to the protocol used by the Emory Viral Vector Core. HEK293 cells were grown and transfected with the capsid and helper plasmids as well as the plasmid of interest. Cells were collect, centrifuged and lysed. The virus was purified using an iodixanol gradient followed by a buffer exchange to PBS plus 0.001% F68 and concentrated in Amicon 15 100,000MWCO concentration units. Quantitative polymerase chain reaction was used to determine viral titers, with sufficient batches on the magnitude of 10^{11} - 10^{12} vg/ml.

SECTION 3: RESULTS

HD MODEL

Huntingtin plasmids containing the human exon 1 gene, with either 20 CAG repeats (HTT-Q20) or 150 CAG repeats (HTT-Q150), were used to establish an *in vitro* model for HD. Both plasmids were tagged with ds-RED to allow for visualization with fluorescent imaging.

Human Embryonic Kidney (HEK293) cells were plated in 96 well plates and transfected the following day with HTT-Q20 or HTT-Q150. There was a distinct difference in expression at 32 hours post-transfection (Figure 5).

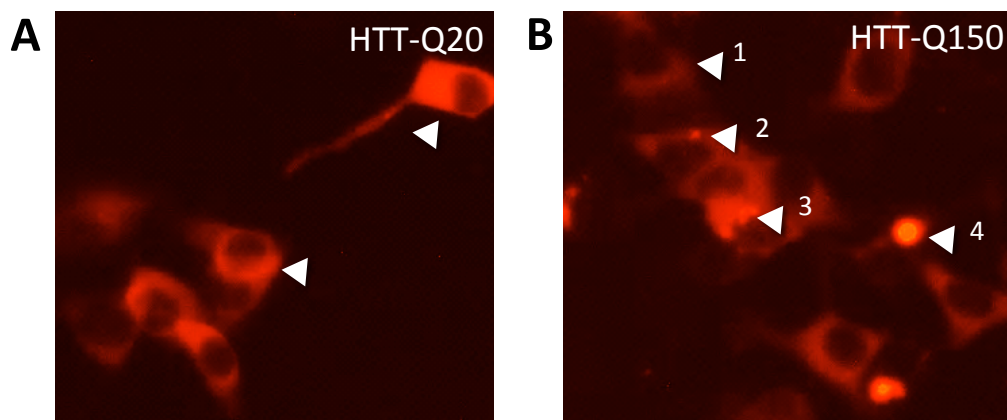


Figure 5: Huntingtin plasmid expression in HEK293 cells 32hr post-transfection.

A) ds-RED-Exon 1 Htt-Q20. Arrows show DsRed expression throughout the cytoplasm. B) dsRED-Exon 1 Htt-Q150. Arrows show varying states of aggregation.

HTT-Q20 expression is observed consistently throughout the cytoplasm with varying intensity. Conversely, cells transfected with HTT-Q150 show the formation of distinct puncta of varying sizes and numbers. Varying stages of aggregation can be observed within neighboring cells (Figure 5B). The cell labeled 1 appears to have expression throughout the cell; however, there is likely the formation of microaggregates that are not yet visible using standard microscopy. In contrast, aggregation has progressed in cell 2, where there seems to be a

nucleation site and formation of a small aggregate. Further exemplifying the heterogeneity of aggregation, cell 3 has numerous aggregates; whereas, there is one large aggregate present in cell 4 with extremely intense dsRED labeling (Figure 5B).

Likewise, this diffuse expression and punctated aggregates in HTT-Q20 and HTT-Q150 respectively, was observed at population level overtime (Figure 6).

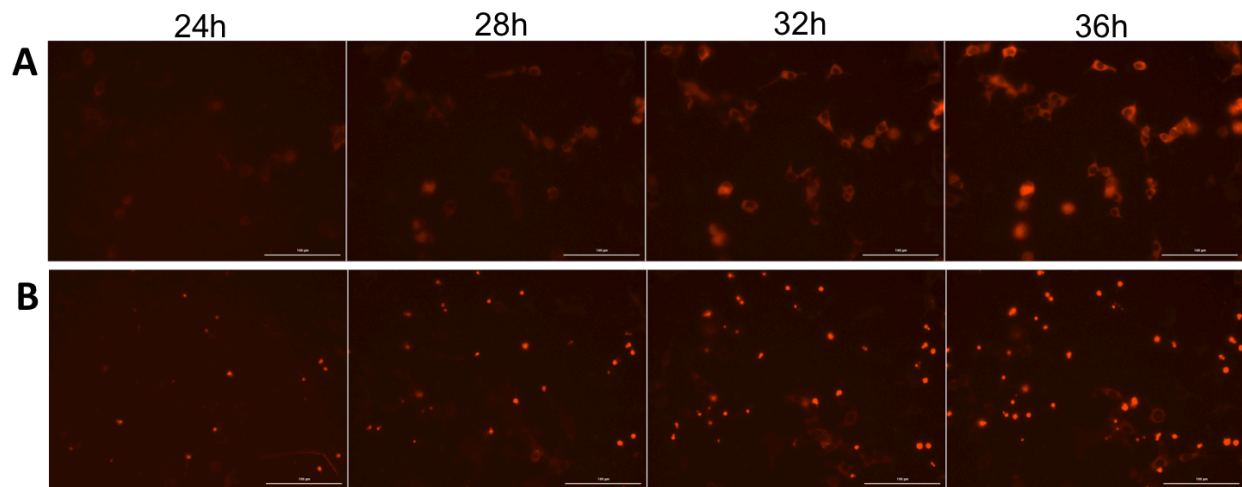


Figure 6: Time-lapse of HTT expression every 4hrs from 24hr to 36hr post-transfection.

A) ds-RED-Exon 1 Htt-Q20 B) dsRED-Exon 1 Htt-Q150

While increase in expression is evident over time, with an increase in both number of cells expressing and intensity, the distribution of HTT-Q20 (Figure 6A) continues to be located throughout the cytoplasm whereas HTT-Q150 (Figure 6B) results in the formation of visible aggregates, a hallmark of mHTT in HD.

TESTING THE ATF4 SENSOR

To test the sensing capabilities of our GTUPR, a plasmid containing the 5'UTR of human *ATF4* gene, the stress-sensitive leader sequence, was cloned into a pAAV-EGFP backbone. The green fluorescent protein (GFP) served as a reporter construct. Its expression was compared to

the constitutively expressed GFP (cGFP). Both plasmids were under the control of the universal chicken- β actin promoter (CBA) (Figure 7).

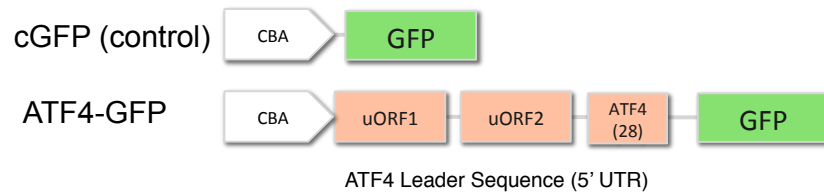


Figure 7: Sensing construct, ATF4-GFP design, and control GFP reporter plasmid.

In unstressed conditions, translation of ATF4 is minimal. Thus, it is expected that the expression of the GFP reporter under the control of the 5' UTR of the ATF4 should also be relatively low. To test our sensing modality, we transfected HEK293 cells with either cGFP or ATF4-GFP. In the cGFP condition, GFP is expressed and visible throughout the cells (Figure 8B). In the ATF4-GFP condition, GFP expression was suppressed (Figure 8B) as compared to the cGFP transfected cells. Expression levels remained constant for both conditions from 24-48 hours post-transfection (Figure 8A).

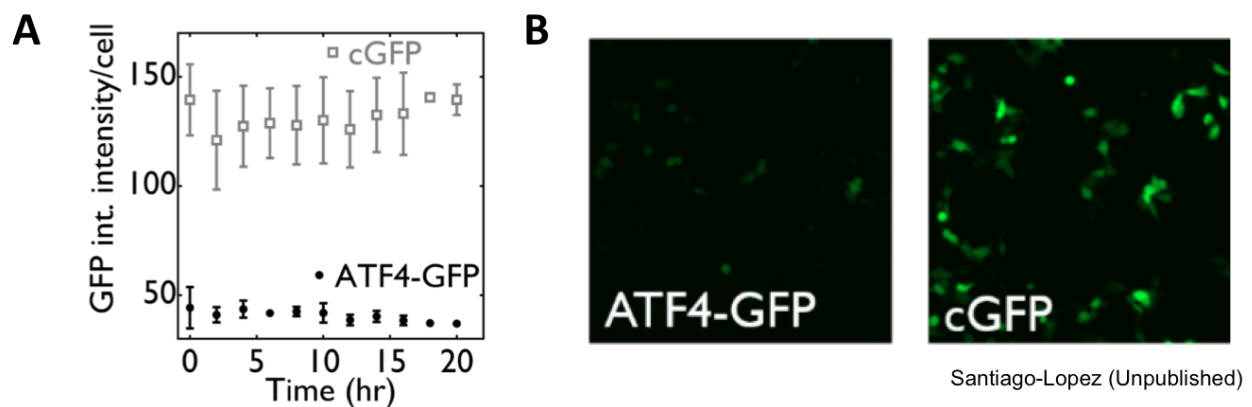


Figure 8: Differential expression of ATF4-GFP versus cGFP. A) The GFP integrated intensity per cell is about 2-fold higher with cGFP than with ATF4-GFP. B) Representative microscopy images taken 24hr post-transfection show much lower levels of GFP under the control of the 5' UTR of the ATF4 gene vs. constitutively expressed GFP.

After determining the baseline expression of the ATF4 construct, we probed the construct's response to stress using tunicamycin (TM), a chemical inducer of ER stress that blocks N-linked glycosylation of proteins. TM leads to hydrophobic residues of native proteins being exposed, and are, hence, recognized by the UPR as misfolded. HEK293 cells expressing ATF4-GFP were treated with varying amounts of TM and GFP expression was monitored over 24 hours. As expected, we observed a strong dose-dependent response, with higher levels of TM inducing more GFP expression (Figure 9A). After 24 hrs, At 24 hr, GFP integrated intensity per cell is increased with increasing dosages of TM, indicating both an increase in expression on a cellular and population basis.

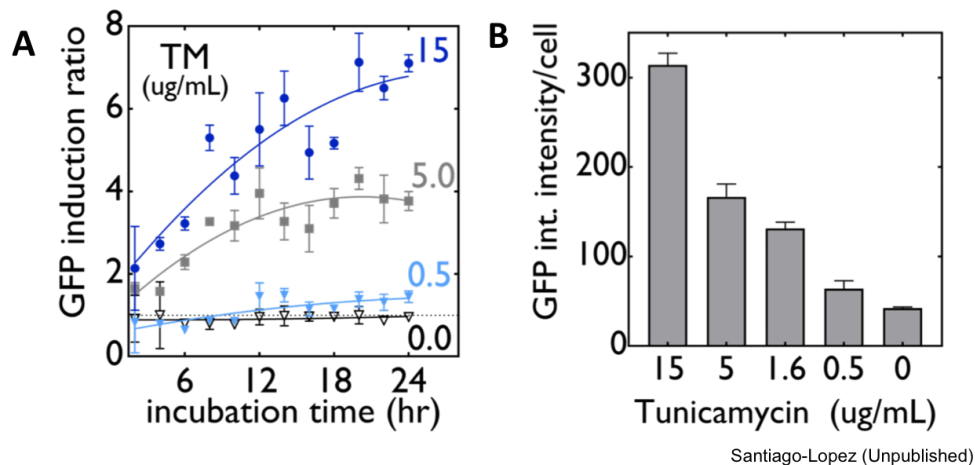


Figure 9: TM-induced increase in ATF4 expression in HEK293. Levels of GFP expression, under the control 5' UTR of ATF4, correlates with TM dosage. A) GFP induction ratio, a measure of integrated intensity of GFP compared to baseline, is reported over time after adding TM. B) GFP integrated intensity per cell is increased with increasing dosages of TM (between 200-350 cells analyzed per condition)

To establish if the stress response and induction of GFP expression were induced by PERK signaling, HEK293 cells transfected with either cGFP or ATF4-GFP were treated with TM in the presence or absence of PERK inhibitor (PERKi). cGFP expression did not appear to be affected by TM or PERKi (Figure 9, bottom row). In contrast, the TM-induced expression of ATF4-GFP was suppressed with the addition of PERKi, indicating the increase in expression is being regulated through the PERK pathway (Figure 9, top row). Basal levels of ATF4-GFP are extremely low and unaffected by PERKi in the absence of induced ER stress.

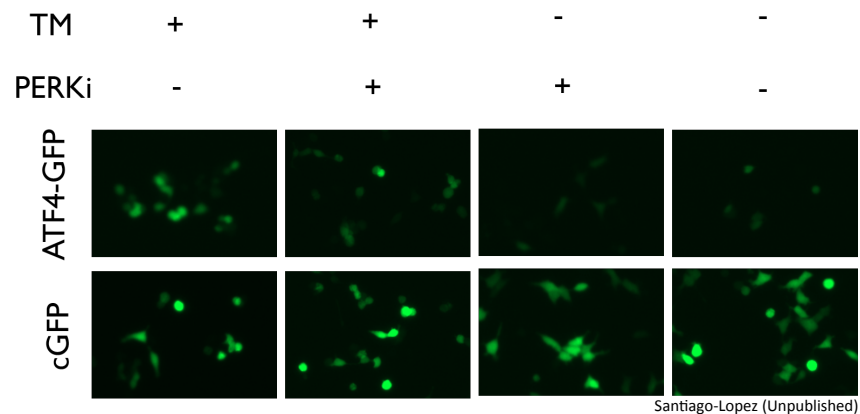


Figure 10: TM-induced increase in ATF4 expression blocked by PERKi in HEK293. The cells were pretreated with 500mM PERKi before TM treatment, 15ug/ml. Images were taken 24hr after the addition of TM.

ATF4 SENSOR IN HD MODEL

Whether this *sensing* construct would be effective in the treatment of HD depends on the differential translation of the transcript in the presence of polyQ aggregates. To determine if HD-related stress activates the gene therapy construct, HEK293 cells were transfected with ATF4-GFP alone, ATF4-GFP + HTT-Q20, or ATF4-GFP + HTT-Q150 and imaged every 3 hours for 48 hr (Figure 10).

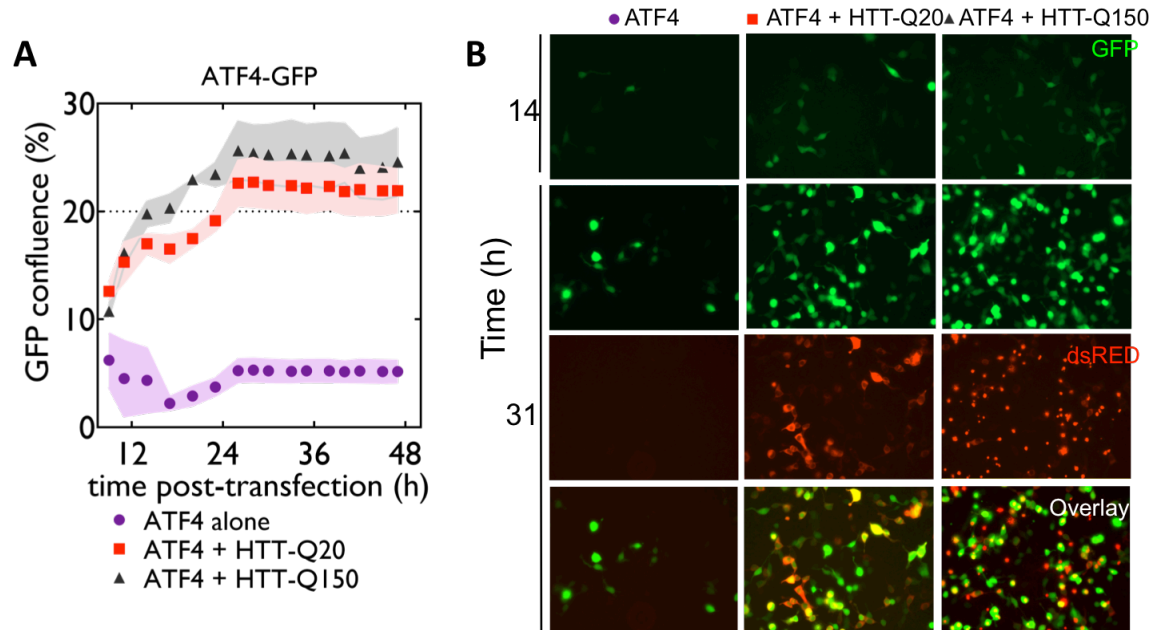


Figure 11: ATF4-GFP induction in response to HTT in HEK293 cells. A) Area of GFP positive cells reported as percent confluence. Each data point is an average of three biological replicates with standard error of the mean (SEM) shown. Nine images were taken per well and averaged at each time point.

As previously shown, cells transfected with the ATF4 plasmid express low levels of GFP. Induction of the ATF4-GFP plasmid is evident when the expression of HTT-Q20 and HTT-Q150 is present. Overtime, the percent area covered by GFP-positive cells, GFP confluence, remained the same for HEK293 cells expressing ATF4-GFP alone. GFP confluence of cells expressing ATF4-GFP with either HTT-Q20 or HTT-Q150 increased over the first 24 hours and plateaued thereafter. A measure of GFP confluence shows induction of the construct in approximately 25% of the image area in the HTT-Q150 expressing cells and slightly lower expression, about 22% confluence in HTT-Q20 expressing cells. This is significantly higher expression than the 5% confluence seen with ATF4 alone. Thus, the difference in translation of the ATF4-GFP construct implies the 5' UTR of ATF4 is sensitive to the stress induced by HTT expression.

MOLECULAR THERAPY, BECLIN-1 EXPRESSION

BECN1, a key regulator of autophagy, was selected to induce and upregulate the autophagy pathway. Both a constitutively expressed and 5' UTR ATF4 controlled BECN1

plasmid were tested and expression monitored via a GFP reporter. We first performed immunocytochemistry to verify the proper expression of BECN1 protein.

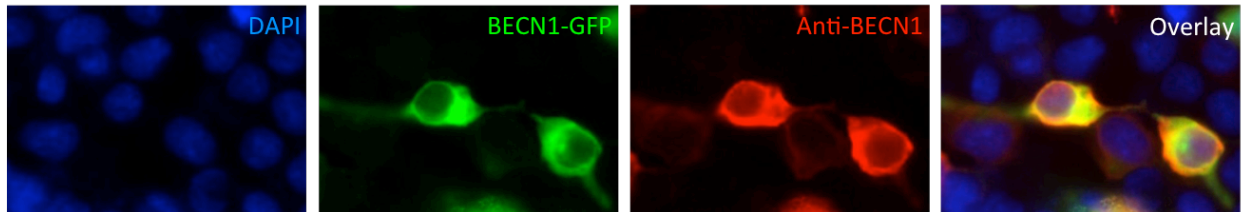


Figure 12: Beclin 1 Immunocytochemistry. HEK293 cells expressing HTT-Q20 and BECN1-GFP were stained 72 hours post-transfection with DAPI and BECN1 antibody tagged with Alexa Fluor[®] 647.

BECN1 immunofluorescence was seen in all the BECN1-GFP expressing cells, confirming the expression of the BECN1 protein fused to GFP (Figure 12). Additionally, some cells were positive of BECN1 when BECN1-GFP expression was not evident. This was likely due to visualization of endogenous BECN1 expression.

RESPONSIVE GENE THERAPY

To assess the efficacy of the responsive gene therapy, we characterized both the differential expression of the construct as well as its effect on HTT expression and aggregation.

HEK293 cells were transfected with ATF4-BECN1 alone or co-transfected with ATF4-BECN1 and HTT-Q20 or HTT-Q150. Following transfection, induction of ATF4-BECN1 expression was monitored overtime. Baseline ATF4-BECN1-GFP expression is low, with an average below 5% GFP confluence (Figure 13A). Upon the introduction of HTT-Q20 and HTT-Q150 expression, ATF4-BECN1-GFP is induced with peak GFP expression occurring between 14-17 hours post-transfection (Figure 13A-B).

In the presence of HTT-Q20 and HTT-Q150, the percent GFP confluence of ATF4-GFP expressing cells remained consistently high after reaching peak expression (Figure 11). Similar to the AFT4-GFP, the percent GFP confluence of ATF4-BECN1-GFP expressing cells peaked

around 14-17 hrs but then decreased over time (Figure 13A). This drop in ATF4 induction suggests that the presence of the BECN1 therapy construct may be influencing UPR-activation by attenuating HTT-induced stress.

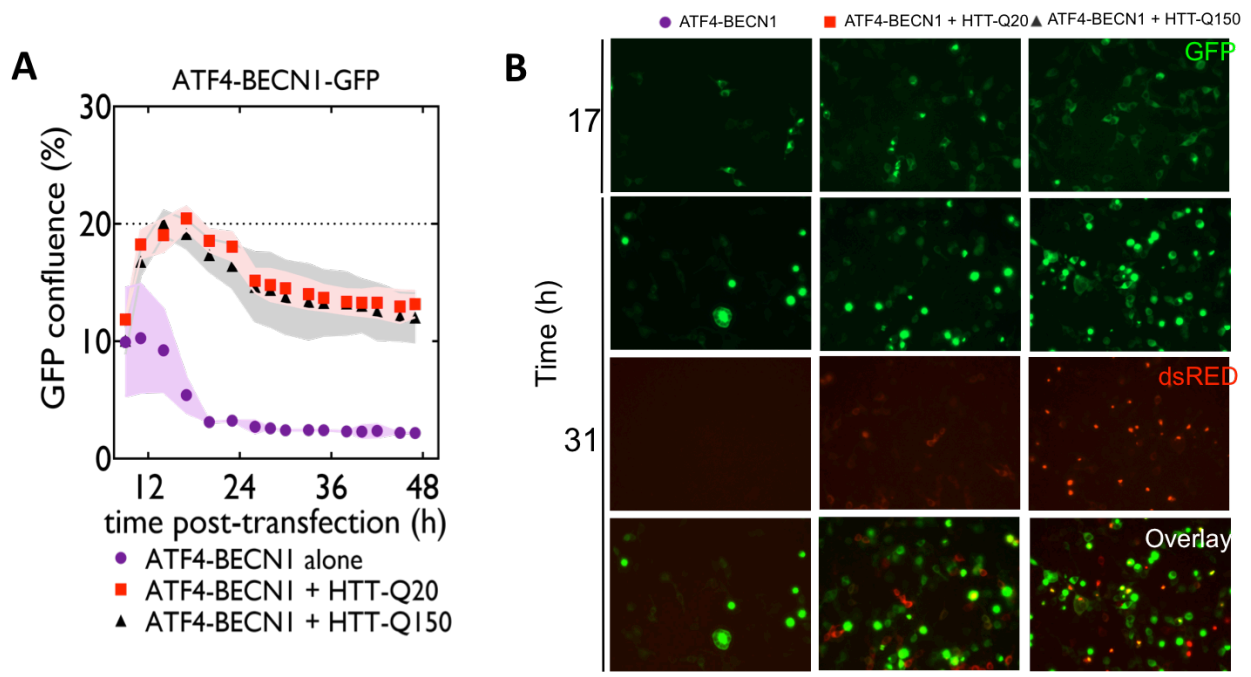


Figure 13: ATF4-BECN1-GFP induction in response to HTT in HEK293 cells. A) Area of GFP positive cells reported as percent confluence. Each data point is an average of three biological replicates with standard error of the mean (SEM) shown. Nine images were taken per well and averaged at each time point.

AFFECT OF BECN1 ON HTT EXPRESSION

The effect of constitutive versus ATF4 controlled BECN1 expression on HTT expression was evaluated. HEK293 cells were transfected with either HTT-Q20 alone or co-transfected with HTT-Q20 and either cBECN1-GFP or ATF4-BECN1-GFP.

All conditions exhibited a similar increase in HTT-Q20 expression (Figure 14) suggesting little to no effect of BECN1 on HTT-Q20 expression. Within the replicates for HTT-Q20 + ATF4-BECN1, there was relatively more variability in levels of HTT expression.

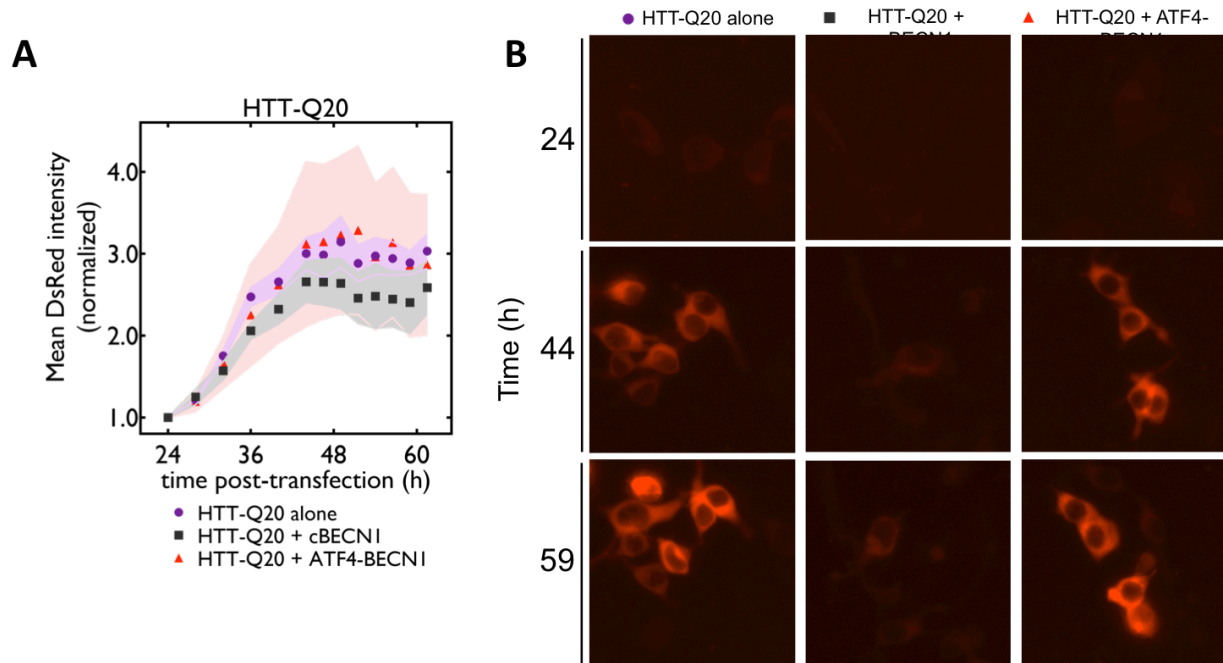


Figure 14: Effect of BECN1 treatment on HTT-Q20 expression in HEK293 cells. Mean integrated intensity of DsRed per object was determined in each image. Four images were taken per well with a minimum of three biological replicates. The average integrated intensity was normalized to that of the first read at 24 hours post-transfection. A) Mean DsRed integrated intensity is reported over time. Error bars shown represent the standard error of the mean (SEM) shown. B) Representative images showing HTT expression at three time points are shown.

This experiment was repeated with the HTT-Q150 construct. In contrast to the HTT-Q20 expressing cells, a drastic suppression of HTT-Q150 expression was observed in the BECN1 treated HTT-Q150 expressing cells (Figure 14). In HTT-Q150 alone condition, HTT expression increased almost 2.5 times (Figure 14A). Whereas, with cells expressing cBECN1 or ATF4-BECN1, expression levels at 24hr were maintained with mild increases in expression below 1.5 times the initial expression levels (Figure 14A). The selective decrease in HTT expression, when the protein contains an elongated polyQ stretch (HTT-Q15), suggests this ATF4 controlled gene therapy may be a promising approach to facilitate the degradation of mutant HTT in HD.

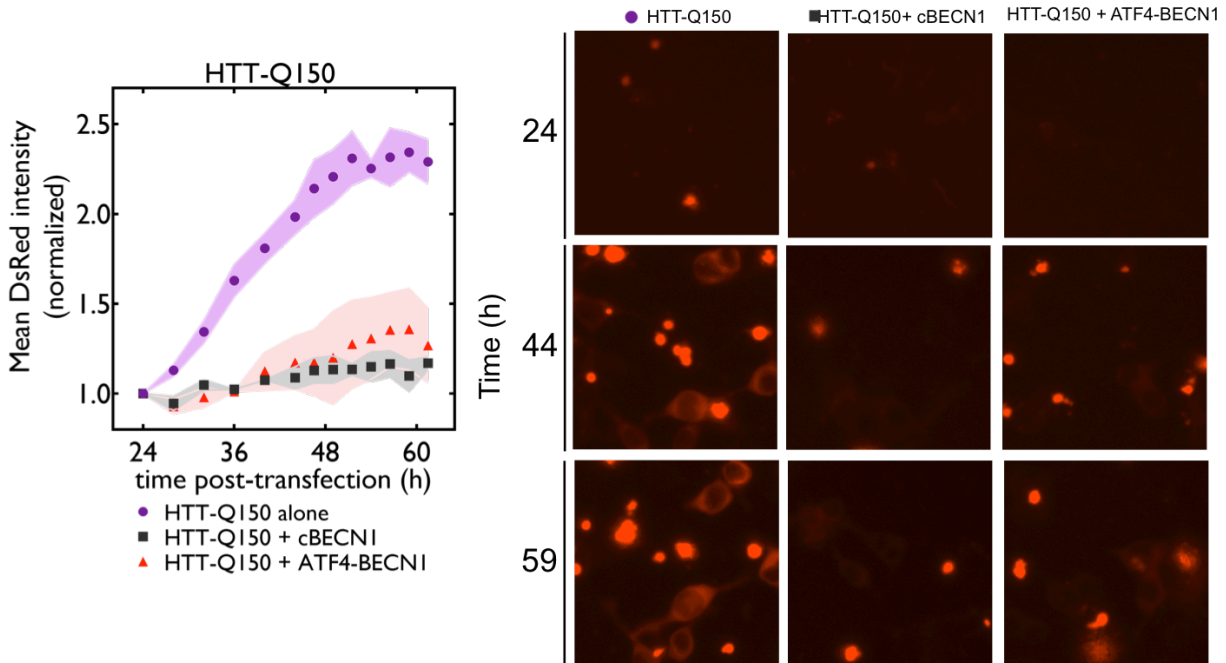


Figure 15: Effect of BECN1 treatment on HTT-Q150 expression in HEK293 cells. Mean integrated intensity of DsRed per object was determined in each image. Four images were taken per well with a minimum of three biological replicates. The average integrated intensity was normalized to that of the first read at 24 hours post-transfection. A) Mean DsRed integrated intensity is reported over time. Error bars shown represent the standard error of the mean (SEM) shown. B) Representative images showing HTT expression at three time points are shown.

We compared the amount of HTT expression with BECN1 treatments at the end of experiments using a one-way ANOVA analysis with Tukey's post-hoc adjustments (Figure 15). No significant difference in dsRed expression was observed between conditions with HTT-Q20 expression (Figure 15A). In contrast, there was a significant decrease in expression in the HTT-Q150 with both BECN1 treatments (Figure 15B; HTT-Q150 + cBECN1: $P = 0.003$, HTT-Q150 + ATF4-BECN1: $P = 0.005$). Both forms of BECN1 expression, cBECN1 and ATF4-BECN1, decreased HTT expression (difference between HTT-Q150 + cBECN1 and HTT-Q150 + ATF4-BECN1 conditions was not significant, $P = 0.9$).

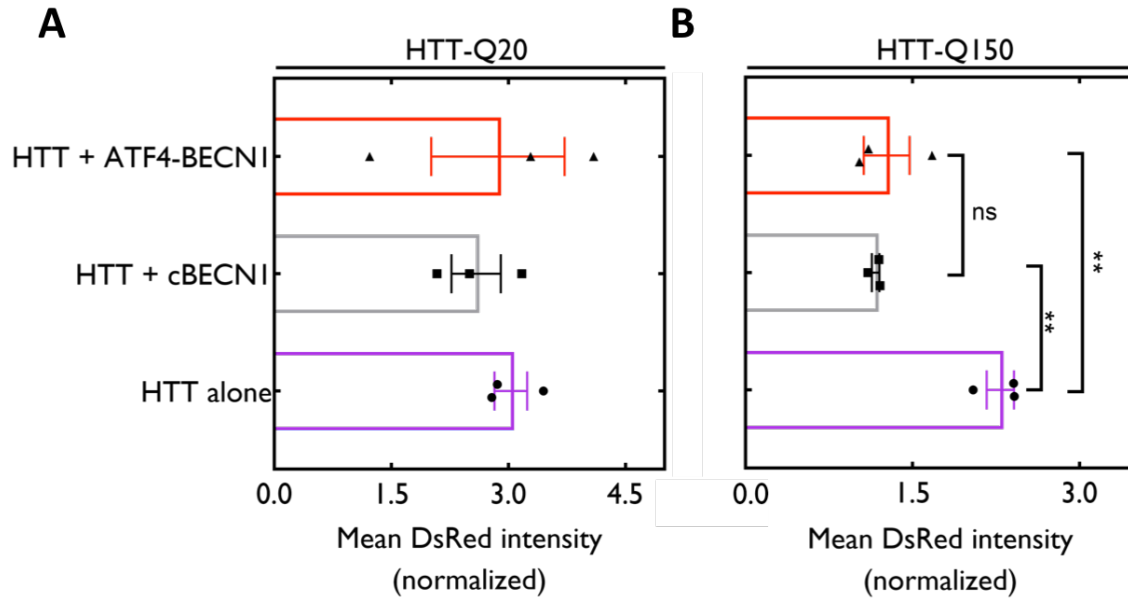


Figure 16: 1-way ANOVA comparing HTT expression in cases of BECN1 treatment at 60hr post-transfection. A) HTT-Q20 expression B) HTT-Q150 expression

EFFECTIVE TRANSDUCTION OF NEURONAL CULTURES WITH ATF4 SENSOR CONSTRUCT

An AAV2-CBA-ATF4-GFP virus was produced to test the *sensing* modality in mouse neuronal culture. Neuronal cultures were transduced with either AAV2-CBA-GFP or AAV2-CBA-ATF4-GFP. Two weeks post infection, AAV2-CBA-GFP showed strong expression in both neurons and glia while only a few cells were expressing AAV2-CBA-ATF4-GFP. Cultures were treated with TM (5ug/ml) to induce ER stress²³ and imaged overtime for 30 hrs. Basal levels of ATF4 were observed in untreated ATF4-GFP transduced cultures (Figure 16B), whereas, the constitutively expressed GFP was strongly visible in neurons and glia (Figure 16C). TM treatment leads to a widespread induction of ATF4-GFP as was seen in the HEK293 cells. However, the TM dose was lethal to the neuronal population and a response was, therefore, only visualized in glia (Figure 16A).

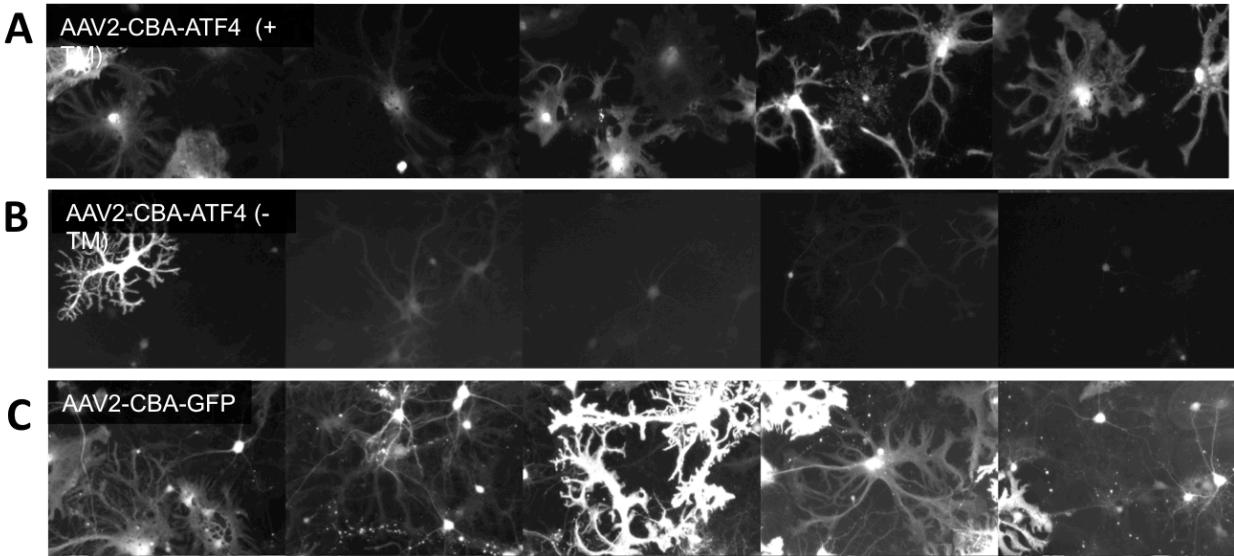


Figure 17: Tunicamycin induction of AAV2-ATF4-GFP construct in neuronal culture. Increased GFP expression in glia 30hr after added TM (5ug/mL), images: 20x magnification A) TM treatment B) No TM added C) GFP control, no TM added

Since HD is characterized by progressive cell death of neurons, the ability of this construct to respond to the presence of unfolded proteins in neurons was specifically of interest. To target neurons only, the promoter was changed from the ubiquitous CBA promoter to the more selective human synapsin I (hSyn) promoter. The control GFP plasmid is expressed in both neurons and glia under the CBA promoter. Expression is excluded from glia under the hSyn promoter, resulting in selective expression of the construct in neurons (Figure 17B).

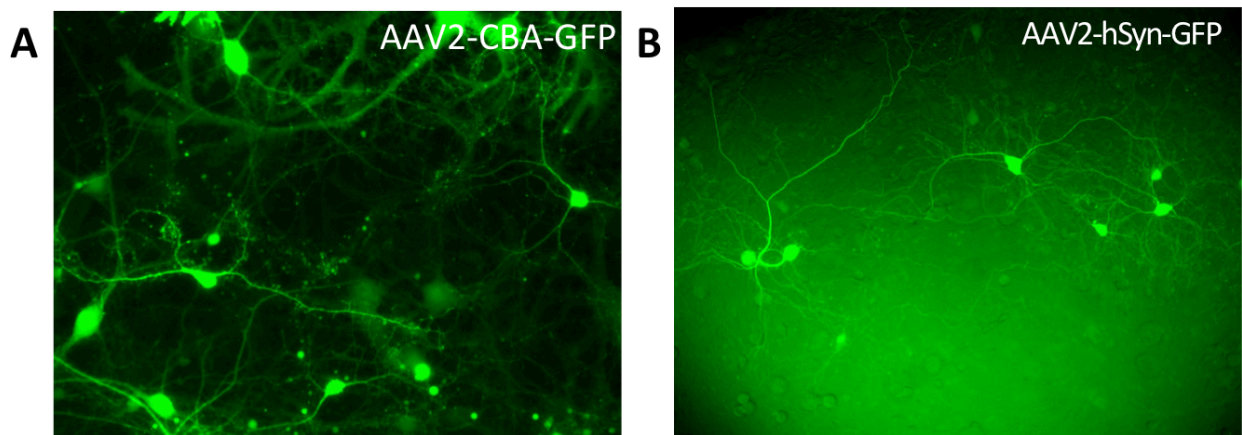


Figure 18: Adeno-associated virus. Difference in expression of control GFP construct under CBA vs. hSyn promoter. A) AAV2-CBA-GFP, B) AAV2-hSyn-GFP.

SECTION 4: DISCUSSION

The goal of this project was to design and test a responsive gene therapy for HD that would function in an autonomous manner and prevent neurodegeneration. Results in HEK293 support the hypothesis that a UPR controlled responsive gene therapy could upregulate autophagy, resulting in a potentially powerful tool for treating HD. Using the 5' UTR of the ATF4 gene, initial experiments have demonstrated that the innate unfolded protein response can be leveraged to control translational dynamics of our gene therapy in a manner dependent on ER stress, induced by the presence of unfolded proteins.

Interestingly, ATF4-GFP expression was induced with HTT-Q150 as well as HTT-Q20. Although GFP expression was higher in HTT-Q150 cells than HTT-Q20 cells, there was still significant induction with this shorter “normal” HTT protein. (Figure 11). The shorter polyQ protein with 20 repeats (the median length within the human population) is not expected to induce ER stress. Nevertheless, these experiments used transfection to introduce the plasmids, under a universal CMV promoter. Under this scenario, HTT-Q20 expression is not regulated as in typical biological conditions. The observed stress response may be linked to the overexpression of HTT-Q20, since intense dsRed expression is indicative of the construct being strongly expressed. Increased protein expression alone puts strain on the cell's protein folding mechanisms.⁴⁹ Additionally, as a molecular scaffold protein, wild-type HTT has numerous protein-protein binding interactions. As a result, it is possible that sufficiently high levels of “normal” forms of HTT protein, also causes cellular dysfunction. This hypothesis could, first, be tested with a more comprehensive immunocytochemical analysis to investigate UPR induction with the expression of both plasmids. Furthermore, in future studies, it will be critical to add a control condition expressing a CMV-dsRed plasmid without the HTT exon 1. Adding this

control would test if the high level of expression of the 20-unit polyQ tract was truly inducing ER stress. Building from this observation, it would be intriguing to look at HTT expression with varying polyQ lengths and examine the effect of repeat length on the induction of our *sensing* modality.

Despite induction of the ATF4-GFP in HTT-Q20 being similar to levels induced with HTT-Q150, as discussed, when the responsive gene therapy construct was introduced, there was a distinct difference in response in terms of HTT expression between plasmids. DsRed expression increased by approximately 2.5-3 times in HTT-Q20, without treatment, with cBECN1, or with ATF4-BECN1. Conversely, cBECN1 and ATF4-BECN1, suppressed HTT-Q150 expression and or promoted clearance of the mutant protein. Further characterization of the status of autophagy, in each experimental condition, may yield insights into the reasons for this differing response.

In addition, it was observed that BECN1 also had the propensity to form puncta. These inclusions were often seemingly colocalized with HTT aggregates confirming previous findings of BECN1 association with HTT.⁹ Reasons for this interaction may be the recruitment of BECN1 to stimulate autophagy and degrade the mHTT and or a degree of mHTT sequestering some BECN1 protein in the aggregates.

cBECN1 and ATF4-BECN1 expression produce similar therapeutic effect, both decreasing HTT-Q150 levels. While the benefit of having the therapy under the control of the ATF4 leader sequence may not be evident in this experiment, this is likely due to the limitations of using HEK293 cells as a model. HEK293 cells are a robust cell line that does not mirror the stress-sensitivity of neurons. In order to evaluate the responsive gene therapy, the construct needs to be introduced into the cell population afflicted in the disease, neurons, more specifically

in medium spiny striatal neurons. Likewise, a more long-term disease model, such as a stable cell line expressing a full-length mHTT, may be more representative of neurodegenerative stress. Neurons may respond differently to the mHTT and are likely more sensitive to the induction and level of autophagy in restoring homeostasis. With the AAV2-hSyn-ATF4-GFP virus, neurons can now be targeted and their stress response characterized. Given the positive results seen in HEK293 cells, both *in vitro* and *in vivo* models need to be explored in choosing a more representative HD model to further explore this innovative and promising new therapeutic avenue.

SECTION 5: CONCLUSION

HD is a devastating genetic condition that induces progressive neurodegeneration. Current treatments fail to effectively address the underlying protein toxicity associated with mHTT expression. Conventional therapies also lack the temporal and dosage control needed to prevent neurodegeneration. Hence, a responsive gene therapy is an optimal method to deliver a therapy for HD, maintaining the cell's ability to degrade protein aggregates and decrease cellular dysfunction, ultimately, preventing neuronal cell death.

Overall, the results are promising, in that an ATF4-5' UTR-controlled gene therapy introduces dynamic control of therapy construct in the context of HD. The closed-loop, self-regulating nature of this construct is unique and powerful. In HEK293 cell characterization studies, the innate detection system of UPR was harnessed and used to control the translation of a gene therapy, inducing expression in the presence of polyQ protein. Additionally, inducing autophagy, by upregulating BECN1, functionally decreased the amount of HTT-Q150 expression and aggregation. This provides a promising platform to test this responsive gene therapy in neuronal models.

SECTION 6: WORKS CITED

1. Chung, C. G., Lee, H. & Lee, S. B. Mechanisms of protein toxicity in neurodegenerative diseases. *Cellular and Molecular Life Sciences* (2018). doi:10.1007/s00018-018-2854-4
2. Frank, S. Treatment of Huntington's Disease. *Neurotherapeutics* (2014). doi:10.1007/s13311-013-0244-z
3. McColgan, P. & Tabrizi, S. J. Huntington's disease: a clinical review. *European Journal of Neurology* (2018). doi:10.1111/ene.13413
4. Weber, J. J., Sowa, A. S., Binder, T. & Hübener, J. From Pathways to Targets: Understanding the Mechanisms behind Polyglutamine Disease. *Biomed Res. Int.* (2014). doi:10.1155/2014/701758
5. Saudou, F. & Humbert, S. The Biology of Huntingtin. *Neuron* (2016). doi:10.1016/j.neuron.2016.02.003
6. Duyao, M. *et al.* Trinucleotide repeat length instability and age of onset in Huntington's disease. *Nat. Genet.* (1993). doi:10.1038/ng0893-387
7. Cisbani, G. & Cicchetti, F. An in vitro perspective on the molecular mechanisms underlying mutant huntingtin protein toxicity. *Cell Death and Disease* (2012). doi:10.1038/cddis.2012.121
8. Metaxakis, A., Ploumi, C. & Tavernarakis, N. Autophagy in Age-Associated Neurodegeneration. *Cells* (2018). doi:10.3390/cells7050037
9. Weber, J. J., Sowa, A. S., Binder, T. & Hübener, J. From pathways to targets: Understanding the mechanisms behind polyglutamine disease. *BioMed Research International* (2014). doi:10.1155/2014/701758
10. Thorburn, A. Autophagy and Its Effects: Making Sense of Double-Edged Swords. *PLoS Biol.* **12**, e1001967 (2014).
11. Shenkman, M., Eiger, H. & Lederkremer, G. Z. Genesis of ER Stress in Huntington's Disease. *Endoplasmic Reticulum Stress in Diseases* (2015). doi:10.1515/ersc-2015-0007
12. Bhattacharyya, K. The story of George Huntington and his disease. *Ann. Indian Acad. Neurol.* **19**, 25 (2016).
13. Atwal, R. S. *et al.* Huntingtin has a membrane association signal that can modulate huntingtin aggregation, nuclear entry and toxicity. *Hum. Mol. Genet.* **16**, 2600–2615 (2007).
14. Rockabrand, E. *et al.* The first 17 amino acids of Huntingtin modulate its sub-cellular localization, aggregation and effects on calcium homeostasis. *Hum. Mol. Genet.* **16**, 61–77 (2007).
15. Ciechanover, A. & Kwon, Y. T. a. Degradation of misfolded proteins in neurodegenerative diseases: therapeutic targets and strategies. *Exp. Mol. Med.* **47**, e147 (2015).
16. Renna, M., Jimenez-Sanchez, M., Sarkar, S. & Rubinsztein, D. C. Chemical inducers of autophagy that enhance the clearance of mutant proteins in neurodegenerative diseases. *Journal of Biological Chemistry* (2010). doi:10.1074/jbc.R109.072181
17. Hetz, C. & Saxena, S. ER stress and the unfolded protein response in neurodegeneration. *Nat. Rev. Neurol.* **13**, 477–491 (2017).
18. Vidal, R., Caballero, B., Couve, A. & Hetz, C. Converging pathways in the occurrence of endoplasmic reticulum (ER) stress in Huntington's disease. *Curr. Mol. Med.* **11**, 1–12 (2011).

19. Kapur, M., Monaghan, C. E. & Ackerman, S. L. Regulation of mRNA Translation in Neurons—A Matter of Life and Death. *Neuron* (2017). doi:10.1016/j.neuron.2017.09.057
20. Leitman, J. *et al.* ER stress-induced eIF2-alpha phosphorylation underlies sensitivity of striatal neurons to pathogenic huntingtin. *PLoS One* (2014). doi:10.1371/journal.pone.0090803
21. Vattam, K. M. & Wek, R. C. Reinitiation involving upstream ORFs regulates ATF4 mRNA translation in mammalian cells. *Proc. Natl. Acad. Sci.* **101**, 11269–11274 (2004).
22. Young, S. K. & Wek, R. C. Upstream open reading frames differentially regulate genespecific translation in the integrated stress response. *J. Biol. Chem.* **291**, 16927–16935 (2016).
23. Cregan, S. P. *et al.* Neuronal Apoptosis Induced by Endoplasmic Reticulum Stress Is Regulated by ATF4-CHOP-Mediated Induction of the Bcl-2 Homology 3-Only Member PUMA. *J. Neurosci.* (2010). doi:10.1523/jneurosci.1598-10.2010
24. Samali, A. *et al.* The integrated stress response. *EMBO Rep.* (2016). doi:10.15252/embr.201642195
25. Qin, Z. H. *et al.* Autophagy regulates the processing of amino terminal huntingtin fragments. *Hum. Mol. Genet.* **12**, 3231–3244 (2003).
26. Glick, D., Barth, S. & Macleod, K. F. Autophagy: Cellular and molecular mechanisms. *Journal of Pathology* (2010). doi:10.1002/path.2697
27. Lipinski, M. M. *et al.* Genome-wide analysis reveals mechanisms modulating autophagy in normal brain aging and in Alzheimer’s disease. *Proc. Natl. Acad. Sci.* **107**, 14164–14169 (2010).
28. Hara, T. *et al.* Suppression of basal autophagy in neural cells causes neurodegenerative disease in mice. *Nature* **441**, 885–889 (2006).
29. Komatsu, M. *et al.* Loss of autophagy in the central nervous system causes neurodegeneration in mice. *Nature* **441**, 880–884 (2006).
30. Wirawan, E. *et al.* Beclin 1: A role in membrane dynamics and beyond. *Autophagy* (2012). doi:10.4161/auto.8.1.16645
31. Nascimento-Ferreira, I. *et al.* Beclin 1 mitigates motor and neuropathological deficits in genetic mouse models of Machado-Joseph disease. *Brain* **136**, 2173–2188 (2013).
32. Nascimento-Ferreira, I. *et al.* Overexpression of the autophagic beclin-1 protein clears mutant ataxin-3 and alleviates Machado-Joseph disease. *Brain* **134**, 1400–1415 (2011).
33. Wu, J. C. *et al.* The regulation of N-terminal Huntingtin (Htt552) accumulation by Beclin1. *Acta Pharmacol. Sin.* **33**, 743–751 (2012).
34. Zheng, S. *et al.* Deletion of the huntingtin polyglutamine stretch enhances neuronal autophagy and longevity in mice. *PLoS Genet.* **6**, (2010).
35. Ashkenazi, A. *et al.* Polyglutamine tracts regulate autophagy. *Autophagy* (2017). doi:10.1080/15548627.2017.1336278
36. Steele, J. W. *et al.* Latrepirdine stimulates autophagy and reduces accumulation of α -synuclein in cells and in mouse brain. *Mol. Psychiatry* **18**, 882–888 (2013).
37. Liu, F. T. *et al.* Fasudil, a Rho kinase inhibitor, promotes the autophagic degradation of A53T α -synuclein by activating the JNK 1/Bcl-2/beclin 1 pathway. *Brain Res.* **1632**, 9–18 (2016).
38. Lu, J. H. *et al.* Isorhynchophylline, a natural alkaloid, promotes the degradation of α -synuclein in neuronal cells via inducing autophagy. *Autophagy* **8**, 98–108 (2012).
39. Shevtsova, Z., Malik, J. M. I., Michel, U., Bähr, M. & Kügler, S. Promoters and serotypes:

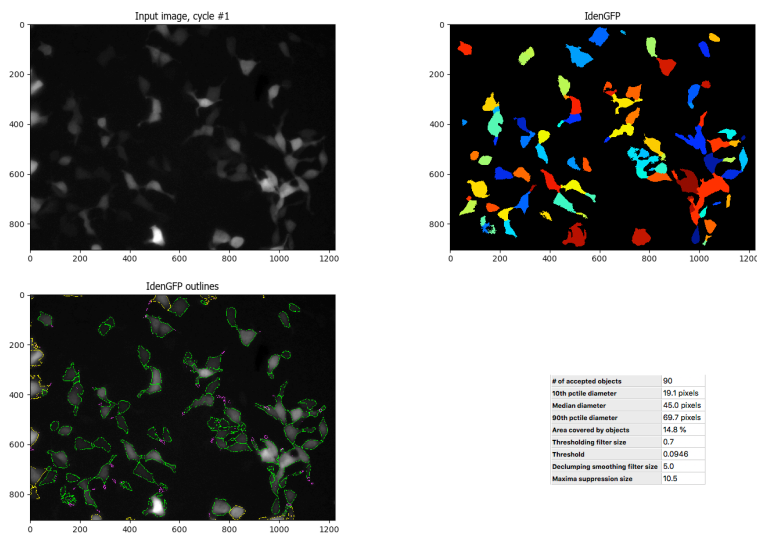
- targeting of adeno-associated virus vectors for gene transfer in the rat central nervous system *in vitro* and *in vivo*. *Exp. Physiol.* **90**, 53–59 (2005).
40. Bally, L., Thabit, H. & Hovorka, R. Glucose-responsive insulin delivery for type 1 diabetes: The artificial pancreas story. *Int. J. Pharm.* **544**, 309–318 (2018).
 41. Schukur, L., Geering, B., Charpin-El Hamri, G. & Fussenegger, M. Implantable synthetic cytokine converter cells with AND-gate logic treat experimental psoriasis. *Sci. Transl. Med.* **7**, 1–12 (2015).
 42. Ausländer, D. *et al.* Sensing and responding to allergic response cytokines through a genetically encoded circuit. *Nat. Commun.* (2017). doi:10.1038/s41467-017-01211-1
 43. Kemmer, C. *et al.* Self-sufficient control of urate homeostasis in mice by a synthetic circuit. *Nat. Biotechnol.* **28**, 355–360 (2010).
 44. Saxena, P., Charpin-El Hamri, G., Folcher, M., Zulewski, H. & Fussenegger, M. Synthetic gene network restoring endogenous pituitary–thyroid feedback control in experimental Graves’ disease. *Proc. Natl. Acad. Sci.* **113**, 1244–1249 (2016).
 45. Sedlmayer, F., Aubel, D. & Fussenegger, M. Synthetic gene circuits for the detection, elimination and prevention of disease. *Nat. Biomed. Eng.* **2**, 399–415 (2018).
 46. Kojima, R., Aubel, D. & Fussenegger, M. Toward a world of theranostic medication: Programming biological sentinel systems for therapeutic intervention. *Adv. Drug Deliv. Rev.* **105**, 66–76 (2016).
 47. Santiago-Lopez A.J., Gutekunst CA., G. R. E. C3 Transferase Gene Therapy for Continuous RhoA Inhibition. in *Rho GTPases. Methods in Molecular Biology*. 267–281 (Humana Press, 2018).
 48. Carpenter, A. E. *et al.* CellProfiler: Image analysis software for identifying and quantifying cell phenotypes. *Genome Biol.* **7**, (2006).
 49. Walter, P. & Ron, D. The unfolded protein response: From stress pathway to homeostatic regulation. *Science* (2011). doi:10.1126/science.1209038

APPENDIX A: CELL PROFILER IMAGE ANALYSIS

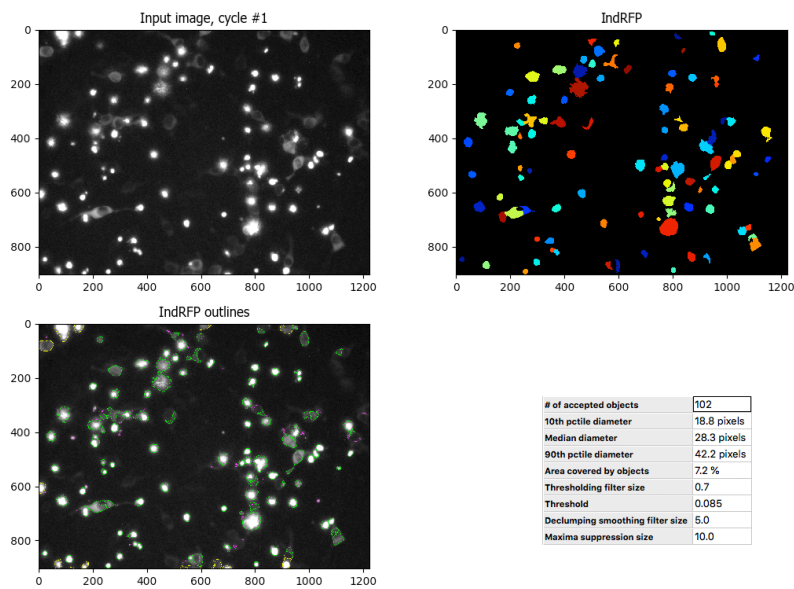
Representative image analysis: using HEK293 cells expressing ATF4-GFP and HTT-Q150

Segmentation

Green Channel



Red Channel



Identified object statistics

Image	Object	Feature	Mean	Median	STD
RFP	IndRFP	IntegratedIntensity	163.588	141.244	131.303
RFP	IndRFP	MeanIntensity	0.206	0.23	0.073
RFP	IndRFP	StdIntensity	0.077	0.101	0.043
RFP	IndRFP	MinIntensity	0.092	0.083	0.016
RFP	IndRFP	MaxIntensity	0.325	0.406	0.119
RFP	IndRFP	IntegratedIntensityEdge	11.414	10.896	4.704
RFP	IndRFP	MeanIntensityEdge	0.116	0.12	0.019
RFP	IndRFP	StdIntensityEdge	0.013	0.012	0.009
RFP	IndRFP	MinIntensityEdge	0.093	0.083	0.016
RFP	IndRFP	MaxIntensityEdge	0.149	0.152	0.039
RFP	IndRFP	MassDisplacement	0.67	0.528	0.614
RFP	IndRFP	LowerQuartileIntensity	0.135	0.139	0.032
RFP	IndRFP	MedianIntensity	0.197	0.187	0.08
RFP	IndRFP	MADIntensity	0.058	0.054	0.041
RFP	IndRFP	UpperQuartileIntensity	0.282	0.311	0.122
RFP	IndRFP	CenterMassIntensity_X	616.909	657.596	316.291
RFP	IndRFP	CenterMassIntensity_Y	464.5	480.089	249.289
RFP	IndRFP	CenterMassIntensity_Z	0.0	0.0	0.0
RFP	IndRFP	MaxIntensity_X	617.0	655.5	316.077
RFP	IndRFP	MaxIntensity_Y	465.304	484.0	249.128
RFP	IndRFP	MaxIntensity_Z	0.0	0.0	0.0

Image	Object	Feature	Mean	Median	STD
GFP	IdenGFP	IntegratedIntensity	186.506	45.939	384.087
GFP	IdenGFP	MeanIntensity	0.081	0.072	0.023
GFP	IdenGFP	StdIntensity	0.009	0.003	0.021
GFP	IdenGFP	MinIntensity	0.066	0.066	0.004
GFP	IdenGFP	MaxIntensity	0.104	0.08	0.073
GFP	IdenGFP	IntegratedIntensityEdge	20.007	13.496	18.341
GFP	IdenGFP	MeanIntensityEdge	0.075	0.072	0.008
GFP	IdenGFP	StdIntensityEdge	0.005	0.002	0.006
GFP	IdenGFP	MinIntensityEdge	0.067	0.066	0.004
GFP	IdenGFP	MaxIntensityEdge	0.089	0.077	0.026
GFP	IdenGFP	MassDisplacement	0.774	0.055	2.435
GFP	IdenGFP	LowerQuartileIntensity	0.074	0.072	0.012
GFP	IdenGFP	MedianIntensity	0.08	0.072	0.02
GFP	IdenGFP	MADIntensity	0.005	0.003	0.008
GFP	IdenGFP	UpperQuartileIntensity	0.086	0.075	0.033
GFP	IdenGFP	CenterMassIntensity_X	629.15	668.997	317.569
GFP	IdenGFP	CenterMassIntensity_Y	399.272	331.748	258.447
GFP	IdenGFP	CenterMassIntensity_Z	0.0	0.0	0.0
GFP	IdenGFP	MaxIntensity_X	628.769	690.0	316.903
GFP	IdenGFP	MaxIntensity_Y	400.769	330.5	260.907
GFP	IdenGFP	MaxIntensity_Z	0.0	0.0	0.0

Overall image statistics

Image	Masking object	Feature	Value
GFP	IdenGFP	Total intensity	24991.83
GFP	IdenGFP	Mean intensity	0.09203568498085032
GFP	IdenGFP	Median intensity	0.074639216
GFP	IdenGFP	Std intensity	0.056963358
GFP	IdenGFP	MAD intensity	0.0028054938
GFP	IdenGFP	Min intensity	0.06032902
GFP	IdenGFP	Max intensity	0.7312337
GFP	IdenGFP	Pct maximal	0.212119538198
GFP	IdenGFP	Lower quartile	0.07183373
GFP	IdenGFP	Upper quartile	0.08614392
GFP	IdenGFP	Total area	271545
GFP		Total intensity	92421.87
GFP		Mean intensity	0.0835266166235576
GFP		Median intensity	0.07183373
GFP		Std intensity	0.04159849
GFP		MAD intensity	0.0030882359
GFP		Min intensity	0.040125098
GFP		Max intensity	0.7312337
GFP		Pct maximal	0.0520562207184
GFP		Lower quartile	0.068745494
GFP		Upper quartile	0.07744471
GFP		Total area	1106496

Image	Masking object	Feature	Value
RFP		Total intensity	81210.75
RFP		Mean intensity	0.07339452650529238
RFP		Median intensity	0.058888238
RFP		Std intensity	0.05297806
RFP		MAD intensity	0.0053054877
RFP		Min intensity	0.029027453
RFP		Max intensity	0.40607885
RFP		Pct maximal	1.37930909827
RFP		Lower quartile	0.054416083
RFP		Upper quartile	0.06502706
RFP		Total area	1106496
RFP	IndRFP	Total intensity	16685.926
RFP	IndRFP	Mean intensity	0.2080331859820716
RFP	IndRFP	Median intensity	0.1652204
RFP	IndRFP	Std intensity	0.111413054
RFP	IndRFP	MAD intensity	0.0605549
RFP	IndRFP	Min intensity	0.071999215
RFP	IndRFP	Max intensity	0.40607885
RFP	IndRFP	Pct maximal	16.2864053461
RFP	IndRFP	Lower quartile	0.11860981
RFP	IndRFP	Upper quartile	0.28299686
RFP	IndRFP	Total area	80208

Objects or Image	Area Occupied	Perimeter	Total Area
IdenGFP	271545	39492.0	1106496

Objects or Image	Area Occupied	Perimeter	Total Area
IndRFP	80208	11799.0	1106496

APPENDIX B: STATISTICAL ANALYSIS

GraphPad software: One-way ANOVA with Tukey's Post-hoc adjustments

1way ANOVA Multiple comparisons									
1	Number of families	1							
2	Number of comparisons per family	3							
3	Alpha	0.05							
4									
5	Tukey's multiple comparisons test	Mean Diff.	95.00% CI of diff.	Significant?	Summary	Adjusted P Value			
6									
7	Untreated vs. cBeclin	1.121	0.5151 to 1.726	Yes	**	0.0031	A-B		
8	Untreated vs. ATF4-Beclin	1.022	0.4163 to 1.628	Yes	**	0.0049	A-C		
9	cBeclin vs. ATF4-Beclin	-0.09871	-0.7044 to 0.507	No	ns	0.8740	B-C		
10									
11									
12	Test details	Mean 1	Mean 2	Mean Diff.	SE of diff.	n1	n2	q	DF
13									
14	Untreated vs. cBeclin	2.29	1.169	1.121	0.1974	3	3	8.029	6
15	Untreated vs. ATF4-Beclin	2.29	1.268	1.022	0.1974	3	3	7.322	6
16	cBeclin vs. ATF4-Beclin	1.169	1.268	-0.09871	0.1974	3	3	0.7072	6